HAL open science

Pitfalls in the frequency response represented onto Polynomial Chaos for random SDOF mechanical systems

Emmanuel Pagnacco, Emmanuelle Sarrouy, Rubens Sampaio, Eduardo Souza de Cursi

To cite this version:

Emmanuel Pagnacco, Emmanuelle Sarrouy, Rubens Sampaio, Eduardo Souza de Cursi. Pitfalls in the frequency response represented onto Polynomial Chaos for random SDOF mechanical systems. Applied Mathematical Modelling, 2017, 52, pp.626-647. 10.1016/j.apm.2017.08.004 . hal-01590996

HAL Id: hal-01590996

https://hal.science/hal-01590996v1

Submitted on 20 Sep 2017

HAL is a multi-disciplinary open access archive for the deposit and dissemination of scientific research documents, whether they are published or not. The documents may come from teaching and research institutions in France or abroad, or from public or private research centers.

L'archive ouverte pluridisciplinaire **HAL**, est destinée au dépôt et à la diffusion de documents scientifiques de niveau recherche, publiés ou non, émanant des établissements d'enseignement et de recherche français ou étrangers, des laboratoires publics ou privés.

Distributed under a Creative Commons Attribution - NonCommercial - NoDerivatives 4.0 International License

Pitfalls in the frequency response represented onto polynomial chaos for random SDOF mechanical systems

E. Pagnacco[a,1,*], E. Sarrouy[b], R. Sampaio[c], E. Souza de Cursi[a]

[a] *Normandie Univ., INSA de Rouen-Normandie, LMN, BP. 8, 76801 St.-Etienne du Rouvray Cedex, France*

[b] *Aix Marseille Univ, CNRS, Centrale Marseille, LMA, Marseille, France*

[c] *PUC-Rio, Mechanical Eng. Dept., Rua Marques de Sao Vicente, 225 22451-900 Rio de Janeiro, RJ Brazil*

Abstract

Uncertainties are present in the modeling of dynamical systems and they must be taken into account to improve the prediction of the models. It is very important to understand how they propagate and how random systems behave. This study aims at pointing out the somehow complex behavior of the structural response of stochastic dynamical systems and consequently the difficulty to represent this behavior using spectral approaches. The main objective is to find numerically the probability density function (PDF) of the response of a random linear mechanical systems. Since it is found that difficulties can occur even for a single-degree-of-freedom system when only the stiffness is random, this work focuses on this application to test several methods. Polynomial Chaos performance is first investigated for the propagation of uncertainties in several situations of stiffness variances for a damped single-degree-of-freedom system. For some specific conditions of damping and stiffness variances, it is found that numerical difficulties occur for the standard polynomial bases near the resonant frequency, where it is generally observed that the shape of the system response PDFs presents multimodality. Strategies to build enhanced bases are then proposed and investigated with varying degrees of success. Finally a multi-element approach is used in order to gain robustness.

Keywords: Dynamic of structure; Frequency Response Function; Random vibration; Propagation of uncertainty; Polynomial Chaos; Multimodality

[*] Corresponding author

Email addresses: `Emmanuel.Pagnacco@insa-rouen.fr` (E. Pagnacco), `emmanuelle.sarrouy@centrale-marseille.fr` (E. Sarrouy), `rsampaio@puc-rio.br` (R. Sampaio), `souza@insa-rouen.fr` (E. Souza de Cursi)

[1] Phone number: 33 2 32 95 97 00

Introduction

This work focuses on distributions of the frequency responses of dynamical systems which have potentially large uncertainties. Common methods for solving stochastic structural dynamics problems are the direct Monte Carlo Simulation (MCS) and the sensitivity-based analysis, such as Neumann or improved perturbation methods. These methods have several drawbacks: MCS is expensive in computing resources for large or complex problems or problems relying on several random variables. Perturbation methods, based on Taylor series expansion, have limited radius of convergence while they do not lead easily to statistical distributions. Hence, efforts are constantly made to explore the suitability of spectral methods, such as the Polynomial Chaos (PC) representation and the Stochastic Reduced Basis Method (SRBM), in order to characterize stochastic mechanical responses. Both of them are non-statistical approaches to represent randomness. Polynomial Chaos representation is based on the "Homogeneous Chaos" theory of Wiener [1], while SRBM is based on the subspace spanned by the considered application [2].

In its original formulation, Wiener defined Homogeneous Chaos theory as the span of Hermite polynomial functionals of Gaussian processes. Next, to model uncertainty in physical applications, the continuous integral form of the Hermite-Chaos has been written in the discrete form of infinite summation which is further truncated for computational purpose. This leads to an approximation technique using PC expansion, where square integrable random variables or processes are represented using an Hilbertian basis consisting of Hermite polynomials of independent standard normal variables. The PC representation provides a complete probabilistic description of the solution. References [3, 4] introduce the moment-based Hermite model for nonlinear random vibration processes and fatigue damage. In these works, the polynomial representation is also generalized to arbitrary polynomials through a procedure analogous to the Gram-Schmidt method. This enables a choice for the representation basis. For instance, Laguerre polynomials have been proposed for positive random processes, associated to chi-square-2 variables. Then, reference [5] combined the Hermite-Chaos representation with the finite element method to model uncertainties encountered in various problems of mechanics. A spectral stochastic finite element method is proposed by using PC representations as trial functions in a Galerkin framework. Next, reference [6] extended this strategy by the introduction of the so-called "generalized Polynomial Chaos" (gPC) that includes a broad family of hypergeometric polynomials, the Askey-scheme [7]. Convergence to any L_2 functional in the L_2 sense of Askey-scheme based PC representation is shown in reference [8]. In contrast, the SRBM chooses a problem-dependent basis. This basis is issued from the vectors which span the stochastic Krylov subspace of the problem. It enables to solve random algebraic systems of equations having non-singular random matrix, such as some of those obtained in structural mechanics.

Hence, in both cases (PC representation and SRBM), exact stochastic solutions are ensured to lie in the – untruncated – subspace generated by the projection basis. But

both these approaches will be computationally ineffective if a large number of vectors is necessary for the representation. This arises for series of slow convergence which implies a high degree of non-linearity in the PC representation. Hence, the accuracy and effectiveness of the polynomial approximation depend upon the terms that are involved in the representation. Some theoretical results of convergence exist. For any arbitrary random process with finite second-order moments, it is found that the Hermite-Chaos representation converges with an optimal convergence rate for Gaussian processes, since the weighting function of Hermite polynomials is the same as the Probability Density Function (PDF) of the Gaussian random variables. But for non-Gaussian processes, the convergence rate may be substantially lower with Hermite polynomials. Similar results occur when considering the Legendre-Chaos for uniform random variables. Convergence rate of gPC representation is studied numerically in references [6, 9], where numerical solutions of stochastic ordinary differential equations with different Wiener-Askey chaos expansions are presented. In these works, the choice of the particular Wiener-Askey chaos is based on the distribution of the input random variable.

More specifically, references [9, 10] address the first two moments of second-order ODE associated to a linear oscillator subject to both random parametric and external forcing excitations having three independent random Gaussian variables using Hermite-Chaos. Ten percent is chosen for the coefficient of variation of the input random variables while the nominal system has five percent of damping ratio. It is shown in [9] that an expansion order up to 14 is required for a specified error in the standard deviation of the response, while the decay rate for the variance is found lower than for the mean. In fact, it is frequent with ODE to observe that the absolute error may increase gradually in time and become unacceptably large for long-term integration [11]. In addition, stochastic regularity of the solution is of the first importance for an efficient approximation using gPC. For discontinuous dependence of the solution on the input random data, gPC may converge slowly or fail to converge even in short-time integration [12].

These phenomenons may indicate that the chosen basis for the representation of random variables is not appropriate. To maintain a spectral polynomial representation basis, [12, 13] introduce a decomposition of the space of random inputs into small elements where gPC is applied, called multi-element gPC method (MEgPC). However, this appears to be not completely sufficient for time dynamical problems, as it demonstrated in reference [11] since the probability density distribution (PDF) of the solution evolves as a function of time. To address this issue, an adaptive gPC method in time is used in [11], where the representation basis evolves in respect to the random solution computed at a previous, known, time step. In reference [14], another way is adopted, based on an understanding of the physics of the system under consideration, when observing the behavior of a two degrees-of-freedom system having a Gaussian stiffness in one spring in order to highlight the main ideas. Some judiciously non-smooth chosen functions, referred as the enrichment functions, are added to the initial Hermite polynomial basis. They are the absolute function, the unit step function and the inverse function.

In [2], it is argued that the convergence of the series is intimately related to the over-

lapping of the probability density functions of the eigenvalues of the stochastic operator for the considered problem. Hence, the practical basis suggested for SRBM in [2] comes from a preconditioned stochastic Krylov subspace, performed from the nominal problem. Numerical studies on frequency response analysis of stochastic structural systems is addressed where 40 Gaussian variables are chosen for the member stiffnesses and masses of a frame structure. In such a situation, the basis is formed by complex vectors. Only the first two moments are studied in this work, showing a degradation in results for large variations of the random variables. However, it is noticed in [15], section 7.1.3.2, that preconditioning from the nominal problem can be a non-optimal choice. Two recent developments are noticeable in SRBM. The first one, proposed in [16], is a hybrid formulation combining SRBM with PC representations to easily tackle problems that necessitate a large number of basis vectors. The second one is a multi-element formulation of SRBM, proposed in [17].

From our experiments in stochastic frequency responses functions for mechanical systems [18, 19, 20, 21, 22], we have found that difficulties can arise with standard PC representation in some situations, while there is no difficulty for others. Difficulties have been observed for several stiffness distributions (namely the Gaussian, uniform and gamma distributions) in single and multiple degrees-of-freedom systems, having or not other random variables (such as random damping for example). Focusing on the single degree-of-freedom (SDOF) system with only one random variable – the spring stiffness – helps to investigate precisely and understand what is happening and under which conditions. Reference [20] conducts numerical investigations for the representation of the SDOF response modulus when Gaussian distribution is considered for the stiffness random variable. Analytical and numerical investigations showed that difficulties with PC representation is intimately related with the potential multimodality that can occur in a specific frequency range, located around the resonant frequency, for some conditions on the variation coefficient of the stiffness when it is compared to the damping ratio.

This study focuses on the stochastic frequency response function of a SDOF linear oscillator whose stiffness is a random variable. To reduce the size of this paper, only Gaussian and uniform distributions are considered. Despite the physical character or not of these distributions, these cases are easier to understand and help to focus on the main ideas. From reference [20], the present work is not only a substantial expansion of it. Indeed:

- The considered problem is now changed for the polynomial chaos representation of the system response, instead of representing only the system response modulus. From our experience, it appears that this situation is more difficult to handle. But such an analysis is essential if we plan to use results of this study for frequency response of general multiple degree-of-freedom systems (see ref. [23]).
- An error indicator based on the Wasserstein metric is proposed here to assess for the quality of polynomial chaos representation for complex random variables, since the considered response has now a real and imaginary part.

- The significant case of a uniform distribution is now considered in addition to the Gaussian distribution for the spring stiffness random variable.
- New combinations are proposed here to form mixed bases and a novel strategy, based on the output variable, is proposed to form an effective PC representation basis.

As a consequence, all results of this study are new. It is organized as follows: Sec. 2 provides first brief recalls over the PC methodology, its alternatives and its numerical implementation. Then, an error indicator is defined over the inverse CDF, which takes into account that a frequency response is not a real variable but a complex quantity. Experiments with PC representation come next. First Hermite-Chaos is tested for the Gaussian stiffness case while Legendre-Chaos is tested for the uniform stiffness case (Sec. 3.1); results are analyzed quantitatively in terms of the error defined over the inverse CDF and qualitatively in terms of CDF and PDF shapes. Then, several other bases are proposed and tested (Sec. 3.2), including the MEgPC approach.

During the revision of this paper came to our attention another nonintrusive approach for making PCE for non-smooth and frequency-dependent system responses, like FRF. The method is very clever and give good results for the computation of FRF in the two cases discussed in [24].

1. Description of the single-degree-of-freedom system

In this section, the stochastic SDOF system is defined and the difficulties associated to its stochastic study when some conditions are met are emphasized using analytical expressions.

1.1. Deterministic system

We consider the following SDOF linear oscillator subject to an external harmonic forcing $q(\omega) = 1$ in the frequency domain [25]:

$$\left(k - \omega^2 + \mathrm{j}c\omega\right) u(\omega) = 1 \tag{1}$$

where $\omega = 2\pi f$ is the circular frequency associated to the frequency f. In this equation, the mass is normalized to unity and k and c are the stiffness and damping parameters of the system. Despite the simplicity, studying such an SDOF system is of interest since it occurs in a similar form when expressing the response of a multiple degrees of freedom system in the modal space. It is sketched in Figure 1.

Since a unit external forcing is considered, the system response $u(\omega)$ is the frequency response function given by:

$$u(\omega) = \frac{1}{k - \omega^2 + \mathrm{j}c\omega} \tag{2}$$

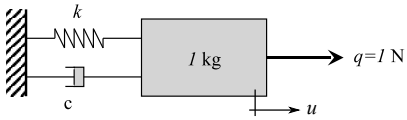

Figure 1: SDOF system

which is a complex quantity such that:

$$\begin{cases} \text{Real}\left[u\left(\omega\right)\right] & = & \left(k-\omega^2\right)\left|u\left(\omega\right)\right|^2 \\ \text{Imag}\left[u\left(\omega\right)\right] & = & -\omega c\left|u\left(\omega\right)\right|^2 \end{cases} \tag{3}$$

where Real $[\bullet]$ and Imag $[\bullet]$ denote the real and imaginary part, respectively, while $|u(\omega)|$ is the response amplitude given by:

$$\left|u\left(\omega\right)\right| = \frac{1}{\sqrt{\left(k-\omega^2\right)^2+\left(\omega c\right)^2}} \tag{4}$$

The response amplitude $|u(\omega)|$ has a maximum at the resonant frequency which is close to the natural frequency of the SDOF system given by:

$$f_0 = \frac{1}{2\pi}\sqrt{k} \tag{5}$$

Hence, the frequency range close to f_0 is often of major interest when a system is designed.

1.2. Stochastic system

Let us consider now a probability space (Ω, $\mathcal{S}$, Prob) with Ω the event space, $\mathcal{S}$ the σ-algebra on Ω, and Prob a probability measure. The SDOF system becomes stochastic if at least one of its parameters is random. Let us consider the situation when only the stiffness k is random. Random variables will be denoted by the capital letter which matches the deterministic variable, hence K in this case. It is such that $K(\varpi) : \Omega \longrightarrow \mathbb{R}$ where $\varpi \in \Omega$. But since the capital letter notation is adopted, the ϖ dependency can now be dropped in the sequel. Let $P_{\mathrm{K}}(k) = \text{Prob}\left[K \leq k\right]$ be the Cumulative Distribution Function (CDF) and $p_{\mathrm{K}}(k) = \frac{\mathrm{d}P_{\mathrm{K}}}{\mathrm{d}k}$ denote the PDF of K having μ_{K} as the mean and σ_{K} as the standard deviation. The domain of K is considered to be an interval having the boundaries k_{inf} and k_{sup} that may or may not belong to the interval depending on the chosen distribution for K. For instance, when the Gaussian random variable is considered, $k \in \left]k_{\text{inf}}, k_{\text{sup}}\right[$ with $k_{\text{inf}} = -\infty$, $k_{\text{sup}} = +\infty$, and the interval is open, the boundaries do not belong to the interval. But when the uniform random variable is considered, $k \in \left[k_{\text{inf}}, k_{\text{sup}}\right]$ with $k_{\text{inf}} = \mu_{\mathrm{K}} - \sqrt{3}\sigma_{\mathrm{K}}$, $k_{\text{sup}} = \mu_{\mathrm{K}} + \sqrt{3}\sigma_{\mathrm{K}}$ and the interval is closed. In this study, the chosen distributions for the random variable K are:

1. the Gaussian, or normal law, which has PDF: $p_{\mathrm{K}}(k) = \dfrac{1}{\sigma_{\mathrm{K}}\sqrt{2\pi}}\exp\left(-\frac{(k-\mu_{\mathrm{K}})^2}{2\sigma_{\mathrm{K}}^2}\right)$; or

2. the uniform law with the PDF: $p_{\mathrm{K}}(k) = \dfrac{1}{k_{\mathrm{sup}} - k_{\mathrm{inf}}} = \frac{1}{2\sqrt{3}\sigma_{\mathrm{K}}}$.

For both of these cases, the natural frequency of the SDOF system becomes a random variable, given by $F_0 = \frac{1}{2\pi}\sqrt{K}$.

Interest arises now in the random system response process $U(\omega)$ which is the frequency response of the system. It is a complex process which depends on the circular frequency $\omega \geq 0$, given by:

$$\left(K - \omega^2 + \mathrm{j}c\omega\right) U(\omega) = 1 \tag{6}$$

that we can compactly rewrite as:

$$U(\omega) = g(K;\, \omega) \tag{7}$$

for:

$$g(K;\, \omega) = \frac{1}{K - \omega^2 + \mathrm{j}c\omega} \tag{8}$$

where g is a non-linear function of its variables. Then, the system response is such that:

$$U(\omega) = \mathrm{Real}\left[U(\omega)\right] + \mathrm{j}\mathrm{Imag}\left[U(\omega)\right] \tag{9}$$

where the real and imaginary parts are random processes:

$$\left\{ \begin{array}{lcl} \mathrm{Real}\left[U(\omega)\right] & = & \left(K - \omega^2\right) \left|U(\omega)\right|^2 \\ \mathrm{Imag}\left[U(\omega)\right] & = & -\omega c \left|U(\omega)\right|^2 \end{array} \right. \tag{10}$$

and the amplitude is:

$$\left|U(\omega)\right| = \frac{1}{\sqrt{\left(K - \omega^2\right)^2 + \left(\omega c\right)^2}} \tag{11}$$

For the uniform stiffness case, it is obvious that $\mathrm{Real}\left[U(\omega)\right]$ and $\mathrm{Imag}\left[U(\omega)\right]$ have finite bounds. For the Gaussian stiffness case, same conclusions arise for $\omega > 0$ since $\left|U(\omega)\right| \in \left]0, \frac{1}{c\omega}\right[$. Moreover, we have also to notice that $\mathrm{Imag}\left[U(\omega)\right]$ is negative in all cases.

Unlike the static case, the PDF of the amplitude of the SDOF system response can have a complex shape for $\omega > 0$, even if a strictly positive damping is considered. Our experience suggests that the complexity is intimately related to the number of statistical modes of the distribution and its potential asymmetry which, in turns, depends on the system parameters and the frequency range of interest. Analytical analyses of $p_{|U|}\left(u, \omega\right)$ for uniform and Gaussian stiffness cases are investigated in references [26, 27, 19]. This reveals that a major parameter is the "normalized coefficient of variation" defined by the ratio $\frac{\sigma_{\mathrm{K}}}{\eta\mu_{\mathrm{K}}}$ where $\eta = \frac{c}{2\sqrt{\mu_{\mathrm{K}}}}$. In fact, when this ratio exceeds a specific value, which depends on the stiffness distribution, several statistical modes may exist for the PDF of the amplitude response over a given frequency range.

Figures 2 and 3 show PDFs of the real and the imaginary parts of the responses of SDOF systems for various normalized coefficient of variation when considering a Gaussian distribution for the stiffness K and a fixed frequency $\omega = \sqrt{\mu_{\mathrm{K}}}$. For a low normalized

coefficient of variation, the PDF of the real part has a bell shape. The PDF of the imaginary part has a comma shape from the supremum bound to the infimum one. Both of them have thus only one statistical mode, center over 0 for the real part and at the infimum bound for the imaginary part. Then, as the normalized coefficient of variation increases, two narrow peaks emerge on either side of the bell shape for the real part, leading to three statistical modes. For a medium normalized coefficient of variation, the bell shape at the middle of the distribution disappears completely while the two narrow peaks amplify, leading to a U shape for the real part. In these conditions, the imaginary part have two statistical modes. For a high normalized coefficient of variation, there is an emergence of two supplementary peaks between the two previous ones for the PDF of the real part of the response. Finally, for a very large normalized coefficient of variation, only the last two peaks subsist in this shape for the real part, while only a narrow peak subsists for the imaginary part.

Figures 4 and 5 show PDFs of the real and the imaginary parts of the responses of SDOF systems for various normalized coefficient of variation when considering a uniform distribution for the stiffness K and a fixed frequency $\omega = \sqrt{\mu_{\mathrm{K}}}$. For a low normalized coefficient of variation, the PDF of the real part has a U shape, having two statistical modes at either bound. But when the normalized coefficient of variation increases, there is an emergence of two supplementary peaks between the two previous ones. Finally, for a very large normalized coefficient of variation, only the last two peaks subsist in this shape for the real part. On another hand, the imaginary parts are quite similar to the ones described for the Gaussian stiffness case.

The shape of the response over all frequencies for an SDOF system can then be quite simple or not, depending on the system parameter values. For a moderately damped system having a non negligible uncertainty, the PDFs of the response can evolve significantly from a simple shape at low frequencies to a complex one near the resonant frequency, while it becomes very simple when reaching high frequencies. This means that the link between the input random variable (the stiffness) and the output random variable (the displacement) can become very non linear. Hence, it can be asserted that a Polynomial Chaos representation of this response may be inefficient near the resonant frequency. In addition, coming back to the results reported in the literature [28, 9, 10], this can explain the bad estimation of the second moment observed in this range of frequencies for a system having these parameters.

In the following, since the stochastic process of interest does not belong to the class of differential stochastic processes, we can focus directly on fixed values for ω. Then, in the sequel, we will not consider the random process $U(\omega)$ but several distinct random variables U_ω.

2. Propagation of uncertainty using a Polynomial Chaos representation

The principle of Polynomial Chaos representation is briefly recalled here for a one dimensional stochastic space, that is when only one generic random variable X is used

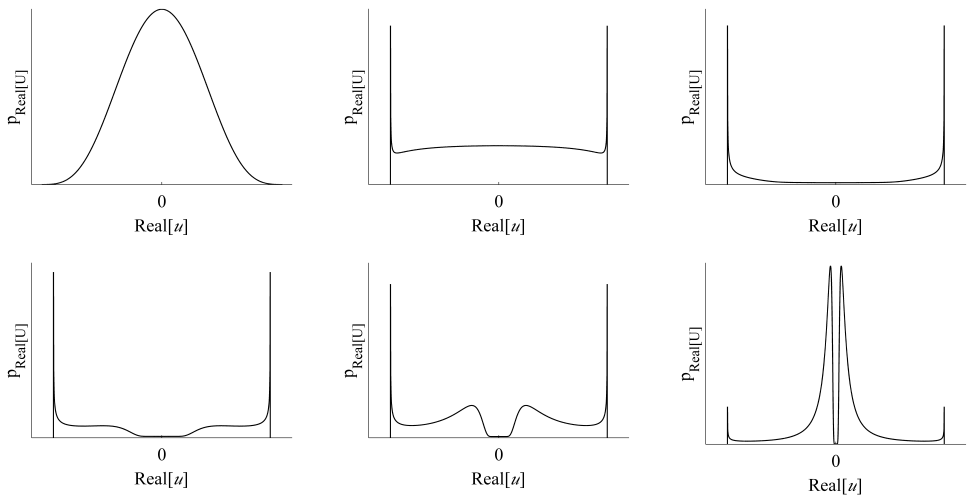

Figure 2: PDFs of the real part of the responses of 6 SDOF systems having the same Gaussian stiffness and different normalized coefficient of variation: from the left most hand, up, to the right most hand, down, they are: 0.33, 0.76, 2.3, 5.7, 11 and 57. The natural frequency of the nominal system is considered.

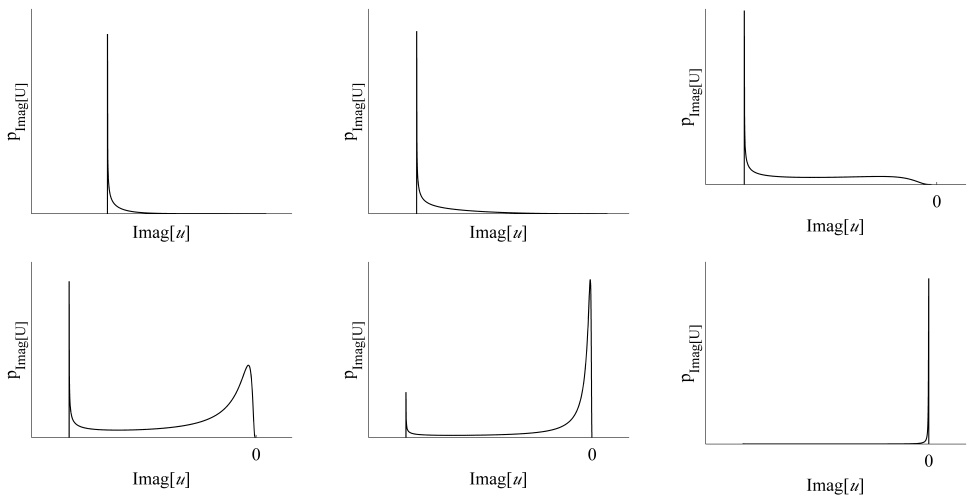

Figure 3: PDFs of the imaginary part of the responses of 6 SDOF systems having the same Gaussian stiffness and different normalized coefficient of variation: from the left most hand, up, to the right most hand, down, they are: 0.33, 0.76, 2.3, 5.7, 11 and 57. The natural frequency of the nominal system is considered.

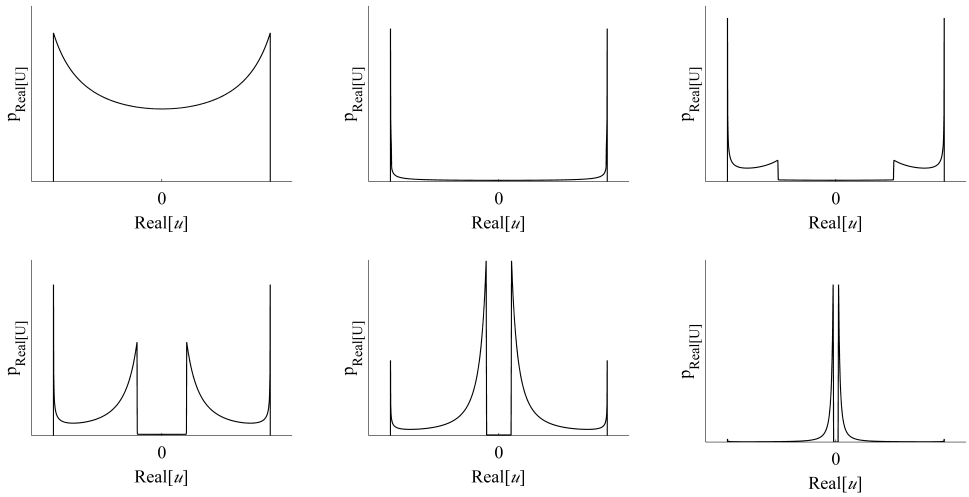

Figure 4: PDFs of the real part of the responses of 6 SDOF systems having the same uniform stiffness and different normalized coefficient of variation: from the left most hand, up, to the right most hand, down, they are: 0.33, 0.76, 2.3, 5.7, 11 and 57. The natural frequency of the nominal system is considered.

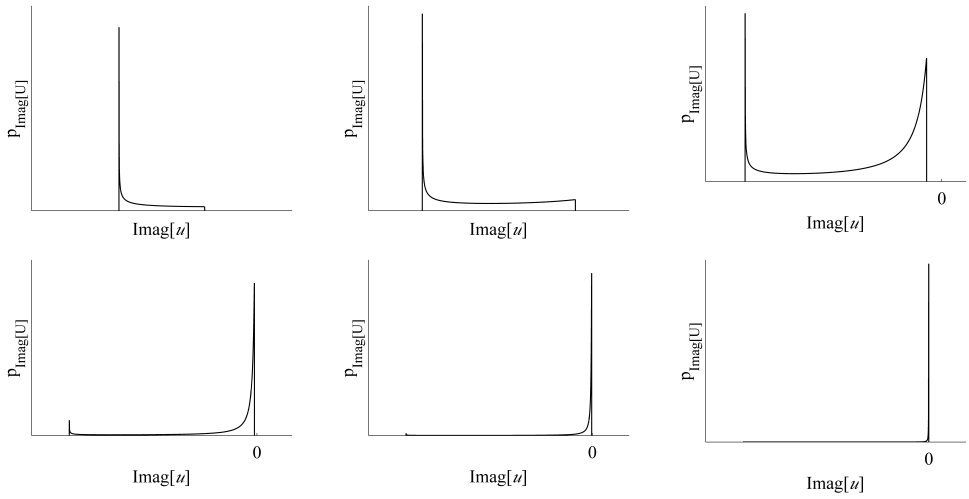

Figure 5: PDFs of the imaginary part of the responses of 6 SDOF systems having the same uniform stiffness and different normalized coefficient of variation: from the left most hand, up, to the right most hand, down, they are: 0.33, 0.76, 2.3, 5.7, 11 and 57. The natural frequency of the nominal system is considered.

to introduce randomness in the system. For a complete presentation of PC method, the reader is invited to refer to the references cited in the introduction. In addition, we introduce in this section the chosen error indicator. Such an indicator is necessary to ensure that a sufficient quality of the PC representations is reached for numerical applications and provides a mean to compare the different methods.

2.1. Principle of Polynomial Chaos representation

Considering a generic model $\mathcal{M}$ and the generic second-order random variable $Z = \mathcal{M}(X)$ such that $\mathrm{E}\left[Z^2\right] < \infty$, the PC representation proposes to express Z as a polynomial series using a set of n_{Z} orthogonal polynomials denoted ψ_r:

$$Z = \sum_{r=0}^{n_{\mathrm{Z}}-1} z_r \psi_r(X) \tag{12}$$

the order n_{Z} being theoretically infinite for general situations. In this work, three bases are considered: the Hermite basis, the Legendre basis and the Chebyshev of 1-*st* kind basis. To anticipate numerical conditioning problems arising with higher orders polynomials, their normalized counterparts are selected. The first five polynomials of these bases are presented in Table 1. The deterministic coefficients z_r now used to represent Z can be evaluated in two ways: using a non-intrusive method or an intrusive one.

The non-intrusive method is based on regression or projection of the sampled model output. By using the orthonormality of the polynomials with respect to the inner product $< \bullet, \bullet >$ in the Hilbert space determined by the support of X, the coefficients z_r given by projection are:

$$z_r = \frac{< Z, \psi_r >}{< \psi_r, \psi_r >} =< Z, \psi_r > \tag{13}$$

for:

$$\langle \bullet, \star \rangle = \mathrm{E}\left[\bullet\star\right] = \int_{x \in \mathcal{D}} \bullet(x)\ \star(x)\, p_{\mathrm{X}}(x)\, \mathrm{d}x \tag{14}$$

such that the orthonormality property reads:

$$\int_{x \in \mathcal{D}} \psi_r(x)\, \psi_q(x)\, p_{\mathrm{X}}(x)\, \mathrm{d}x = \begin{cases} 0 & \text{if} \quad r \neq q \\ 1 & \text{if} \quad r = q \end{cases} \tag{15}$$

where p_{X} is the weight function or PDF of the input variable X and $\mathcal{D}$ is its support. They are given in Table 2.

Thus, when a PC representation is needed for the stiffness K, the best choice is to select the Hermite basis for the Gaussian stiffness case while the choice is the Legendre basis for the uniform stiffness case. Indeed, both of them are obtained by a linear transformation $\mathcal{T}_K$ of the input variable[1]. This leads obviously to an order 1 for the PC representation

[1]For instance, if we consider the Gaussian stiffness case and a normal centered reduced variable X, we have: $K = \mu_{\mathrm{K}} + \sigma_{\mathrm{K}} X = \mathcal{T}_{\mathrm{K}}(X)$. It is: $K = \mu_{\mathrm{K}} + \sqrt{3}\sigma_{\mathrm{K}} X = \mathcal{T}_{\mathrm{K}}(X)$ for the uniform stiffness case and a uniform variable X defined on $[-1, 1]$.

Order p	Hermite polynomials	Legendre polynomials	Chebyshev of 1-st kind
0	1	1	1
1	x	$\sqrt{3}x$	$\frac{1}{\sqrt{2}}x$
2	$\frac{1}{\sqrt{2}}\left(x^2-1\right)$	$\frac{\sqrt{5}}{2}(3x^2-1)$	$\frac{1}{\sqrt{2}}\left(2x^2-1\right)$
3	$\frac{1}{\sqrt{6}}\left(x^3-3x\right)$	$\frac{\sqrt{7}}{2}(5x^3-3x)$	$\frac{1}{\sqrt{2}}\left(4x^3-3x\right)$
4	$\frac{1}{2\sqrt{6}}\left(x^4-6x^2+3\right)$	$\frac{\sqrt{9}}{8}(35x^4-30x^2+3)$	$\frac{1}{\sqrt{2}}\left(8x^4-8x^2+1\right)$

Table 1: First five polynomials of the three considered bases

	Hermite	Legendre	Chebyshev of 1-st kind
p_{X}	$\frac{1}{\sqrt{2\pi}}\,\mathrm{e}^{-\frac{1}{2}x^2}$	$\frac{1}{2}$	$\frac{1}{\pi\sqrt{1-x^2}}$
$\mathcal{D}$	$\mathbb{R}$	$[-1,\,1]$	$[-1,\,1]$

Table 2: PDFs associated to the polynomial bases for their orthogonality property

of K. It is $K=\sum_{r=0}^{1}k_r\psi_r(X)$ in both the stiffness cases with:

$$k_r=\mathrm{E}\left[\psi_r(X)K\right]=\int_{x\in\mathcal{D}}\psi_r(x)\,\mathcal{T}_{\mathrm{K}}(x)\,p_{\mathrm{X}}(x)\,\mathrm{d}x=\begin{cases}\mu_{\mathrm{K}} & \text{for}\quad r=0\\ \sigma_{\mathrm{K}} & \text{for}\quad r=1\end{cases}\tag{16}$$

But to find the PC representation in more complex, non-linear situations, as for the stiffness K when considering non-optimal bases, or as for the system response U_ω for a given circular frequency ω with any bases, readily expressions are not available. For instance, let us consider the PC representation of U_ω such that $U_\omega=\sum_{q=0}^{n_{\mathrm{U}}-1}u_q\psi_q(X)$ where:

$$u_q=\mathrm{E}\left[\psi_q U_\omega\right]=\int_{x\in\mathcal{D}}\psi_q(x)\,g(x;\,\omega)\,p_{\mathrm{X}}(x)\,\mathrm{d}x\tag{17}$$

and:

$$g(x;\,\omega)=\frac{1}{\mathcal{T}_{\mathrm{K}}(x)-\omega^2+\mathrm{j}c\omega},\qquad\text{for}:\ \mathcal{T}_{\mathrm{K}}(x)=P_{\mathrm{K}}^{-1}\left(P_{\mathrm{X}}(x)\right).\tag{18}$$

Evaluating the expectation – or inner product – of Eq. (17) necessitates a numerical method. Gauss quadrature formulas can be used for this:

$$\int_{x\in\mathcal{D}}\psi_q(x)\,g(x;\,\omega)\,p_{\mathrm{X}}(x)\,\mathrm{d}x=\sum_{i=1}^{n_{\mathrm{G}}}w_i\psi_q(x_i)g(x_i;\,\omega)\tag{19}$$

where n_{G} is the number of x_i evaluation points for the numerical quadrature and w_i are their weights. The isoprobabilistic transformation is then evaluated for a given value x_i.

The intrusive method follows a Galerkin approach: expression (12) is introduced in the model governing Z and the result is projected onto the set of orthogonal polynomials ψ_r. Then, for the studied mechanical system, it is necessary to consider Eq. (6) to define the error $R\left(X\right)$ as:

$$R(X)=\left(K-\omega^2+\mathrm{j}c\omega\right)U_\omega(X)-1\tag{20}$$

where the output variable U_ω is represented as:

$$U_\omega = \sum_{q=0}^{n_{\mathrm{U}}-1} u_q \psi_q(X) = \mathbf{\Psi}\left(X\right)\mathbf{u} \tag{21}$$

with the complex coefficients u_q for a basis $\mathbf{\Psi} = \{\psi_0,\, \psi_1,\, \ldots,\, \psi_{n_{\mathrm{U}}-1}\}$ composed of polynomials up to degree $n_{\mathrm{U}}-1$. Then, the vector $\mathbf{u}$ of unknown coefficients is obtained by projecting the error onto the trial basis:

$$\langle R\left(X\right), \psi_q(X)\rangle = \int_{x\in\mathcal{D}} R\left(x\right)\psi_q(x) p_{\mathrm{X}}\left(x\right)\,\mathrm{d}x = 0, \qquad q = 1,\, 2,\, \cdots,\, n_{\mathrm{U}} \tag{22}$$

This leads to the following set of n_{U} equations for the estimation of $\mathbf{u}$:

$$\left(\mathrm{E}\left[\mathbf{\Psi}^{\mathrm{T}} K \mathbf{\Psi}\right] + \left(\mathrm{j}c\omega - \omega^2\right)\mathrm{E}\left[\mathbf{\Psi}^{\mathrm{T}}\mathbf{\Psi}\right]\right)\mathbf{u} = \mathrm{E}\left[\mathbf{\Psi}^{\mathrm{T}}\right] \tag{23}$$

where $\mathrm{E}\left[\mathbf{\Psi}^{\mathrm{T}}\mathbf{\Psi}\right] = \mathbf{I}$ for normalized polynomials. It is a linear deterministic system which can be developed as:

$$\sum_{q=0}^{n_{\mathrm{U}}-1}\left(\mathrm{E}\left[\psi_i K \psi_q\right] + \left(\mathrm{j}c\omega - \omega^2\right)\mathbf{I}\right)u_q = \mathrm{E}\left[\psi_i\right] \qquad i = 0, \ldots,\, n_{\mathrm{U}}-1 \tag{24}$$

or, more compactly:

$$\left(\mathcal{K} + \left(\mathrm{j}c\omega - \omega^2\right)\mathbf{I}\right)\mathbf{u} = \mathbf{f} \tag{25}$$

where:

$$\mathcal{K} = \begin{bmatrix} \mathrm{E}\left[\psi_0 K \psi_0\right] & \mathrm{E}\left[\psi_0 K \psi_1\right] & \cdots \\ \mathrm{E}\left[\psi_0 K \psi_1\right] & \mathrm{E}\left[\psi_1 K \psi_1\right] & \\ \vdots & & \ddots \end{bmatrix} \qquad \mathbf{u} = \begin{bmatrix} u_0 \\ u_1 \\ \vdots \end{bmatrix} \qquad \mathbf{f} = \begin{bmatrix} \mathrm{E}\left[\psi_0\right] \\ \mathrm{E}\left[\psi_1\right] \\ \vdots \end{bmatrix} \tag{26}$$

A further step, optional, consists in using in the previous expressions a polynomial representation of K when using the polynomial basis $\mathbf{\Phi} = \{\phi_0,\, \phi_1,\, \ldots,\, \phi_{n_{\mathrm{U}}-1}\}$, such that $K = \sum_{r=0}^{n_{\mathrm{K}}-1} k_r \phi_r\left(Y\right)$ where Y is the random variable associated to polynomials ϕ_r. Then, $Y = \mathcal{T}_{\mathrm{Y}}\left(X\right)$ for the isoprobabilistic transformation $\mathcal{T}_{\mathrm{Y}}$ defined by $\mathcal{T}_{\mathrm{Y}}(x) = P_{\mathrm{Y}}^{-1}\left(P_{\mathrm{X}}(x)\right)$ where P_{X} denotes the CDF of X and P_{Y} the CDF of Y. This leads to:

$$\left(\sum_{r=0}^{n_{\mathrm{K}}-1} k_r \mathrm{E}\left[\mathbf{\Psi}^{\mathrm{T}}\phi_r\mathbf{\Psi}\right] + \left(\mathrm{j}c\omega - \omega^2\right)\mathbf{I}\right)\mathbf{u} = \mathrm{E}\left[\mathbf{\Psi}^{\mathrm{T}}\right] \tag{27}$$

where:

$$k_r = \mathrm{E}\left[\phi_r K\right] = \int_{x\in\mathcal{D}} \phi_r(\mathcal{T}_{\mathrm{Y}}(x))\,\mathcal{T}_{\mathrm{K}}(x)\,p_{\mathrm{X}}(x)\,\mathrm{d}x$$

This strategy corresponds to the one proposed in [5, 6] if the output variable U_ω is expanded onto the same basis than the variable K, *i.e.* if ϕ_r and ψ_r are chosen identical.

In this situation, Eq. (23) becomes:

$$\left(\sum_{r=0}^{n_{\mathrm{K}}-1} k_r \mathrm{E}\left[\mathbf{\Psi}^{\mathrm{T}}\psi_r\mathbf{\Psi}\right] + \left(\mathrm{j}c\omega - \omega^2\right)\mathbf{I}\right)\mathbf{u} = \mathrm{E}\left[\mathbf{\Psi}^{\mathrm{T}}\right] \tag{28}$$

Hence, in the sequel, we referred the equations system (27) as a "two bases intrusive formulation", while the equations system (28) corresponds to the "standard intrusive formulation".

Thus, the main difference between both methods is that the intrusive methods provide a set of coupled algebraic equations and often require a special implementation while the non-intrusive approach determines the set of coefficients z_r one after the other in an independent manner and reuses existing codes to evaluate Z values needed for the quadrature. Moreover, it has to be noticed that a limited expansion where higher orders are truncated leads generally to an approximation. Then, a major remark concerns the interpretation of the coefficients u_q: while the mean of the real part and the mean of the imaginary part of U_ω are both given by the real part and the imaginary part of the complex coefficient u_0, the mean of $|U_\omega|$ as well as higher order moments of $|U_\omega|$ are expressed as a combination of all the coefficients u_q. Hence, a non appropriate order of truncation or a misevaluation of the coefficients of the representation leads implacably to a drift in these moments. As a consequence, fidelity in the PC representation of the PDFs of the real and imaginary parts of U_ω is necessary to correctly estimate mean and variance of the amplitude in a post-processing phase.

2.2. Error indicator

It is necessary to define an error indicator ϵ for the evaluation of the quality of the PC representation. We choose to base it on the L_2 Wasserstein metric which is a distance function defined between two probability measures Prob_1 and Prob_2. Indeed, L_2 Wasserstein metric can be defined by:

$$\mathcal{W}\left(\mathrm{Prob}_1, \mathrm{Prob}_2\right) = \inf\left\{\sqrt{\mathrm{E}\left[(Z_1 - Z_2)^2\right]}; \mathcal{L}(Z_1) = \mathrm{Prob}_1, \mathcal{L}(Z_2) = \mathrm{Prob}_2\right\} \tag{29}$$

where $\mathcal{L}\left[Z\right]$ denotes the law associated to real random variable Z. For a practical evaluation, it can be rewritten as [29]:

$$\mathcal{W}^2\left(\mathrm{Prob}_1, \mathrm{Prob}_2\right) = \int_0^1 \left(P_{Z_1}^{-1}(z) - P_{Z_2}^{-1}(z)\right)^2 \mathrm{d}z \tag{30}$$

and a normalized version is obtained when dividing it by the variance of Z_1 [29]. Since, the Wasserstein metric is a natural way to compare the probability distributions of two real variables Z_1 and Z_2, it can be used as an error indicator if one of them is a reference random variable. To handle complex random variables, we propose to use the following

error expression in this study:

$$\begin{aligned}\epsilon^2 = \quad & \tfrac{1}{\sigma_{\mathrm{R}}^2}\int_0^1 \left(P^{-1}_{\mathrm{Real}[Z_1]}(z) - P^{-1}_{\mathrm{Real}[Z_2]}(z)\right)^2 \mathrm{d}z \\ & + \tfrac{1}{\sigma_{\mathrm{I}}^2}\int_0^1 \left(P^{-1}_{\mathrm{Imag}[Z_1]}(z) - P^{-1}_{\mathrm{Imag}[Z_2]}(z)\right)^2 \mathrm{d}z\end{aligned} \tag{31}$$

where σ_{R}^2 is the variance of the real part of Z_1 and σ_{I}^2 is the variance of its imaginary part.

In this work, this error indicator is used to compare a reference random variable Z_1 to its representation Z_2 given by the PC, where the reference random variable Z_1 is given either analytically or from MCS. Numerically, we have required that ϵ must be less or equal to 5.10^{-4} to ensure an extreme high fidelity in the representation of the random variable Z_2. In industrial applications, the reference variable would not be known and the PC representation is used to approximate it, while it is desirable to limit the amount of computations. In such cases, we assess that the proposed indicator can be used to test the convergence of the representation, by comparing two random variables Z_1 and Z_2 given by PC representations truncated at different orders.

3. Application to SDOF system response

As mentioned previously, the SDOF system response distribution strongly depends on the ratio between the stiffness dispersion (measured by $\sigma_{\mathrm{K}}/\mu_{\mathrm{K}}$ ratio) and the damping (*i.e.* c); or, alternatively, it depends on the ratio $\sigma_{\mathrm{K}}/\mu_{\mathrm{K}}$ and the damping ratio (*i.e.* η). Hence, several configurations must be investigated numerically to test the effectiveness of PC representations. Then, for experimentations, it is possible to fix the damping and vary the coefficient of variation or vice versa. Considered numerical values are arbitrarily chosen such that: $\mu_{\mathrm{K}} = 3500$ N/m and $\eta_m \in \{0.35, 0.05, 0.02\}$ for both Gaussian and uniform stiffness cases. However, $\sigma_{\mathrm{K}} = 400$ N/m is chosen for the Gaussian stiffness case while it is $\sigma_{\mathrm{K}} = 700$ N/m for the uniform stiffness case. This leads to normalized coefficients of variation $\frac{\sigma_{\mathrm{K}}}{\eta_m \mu_{\mathrm{K}}} \simeq \{0.33, 2.3, 5.7\}$ for the Gaussian stiffness case while it is $\frac{\sigma_{\mathrm{K}}}{\eta_m \mu_{\mathrm{K}}} \simeq \{0.57, 4, 10\}$ for the uniform stiffness case.

3.1. Standard PC representation of the response

Let us first consider the standard PC representation for the SDOF system, where standard stands for the polynomial basis chosen accordingly with the one for the stiffness variable: To represent the random response, Hermite polynomial basis is considered for the Gaussian stiffness, while Legendre polynomial basis is considered for the uniform stiffness. This choice follows the recommendations given in [6]. The reason comes from the fact that K admits an exact representation with two terms in both of these cases. An intrusive approach is adopted in what follows; using Eq. (23) or Eq. (27) for the evaluation of polynomial coefficients will obviously lead to the same results.

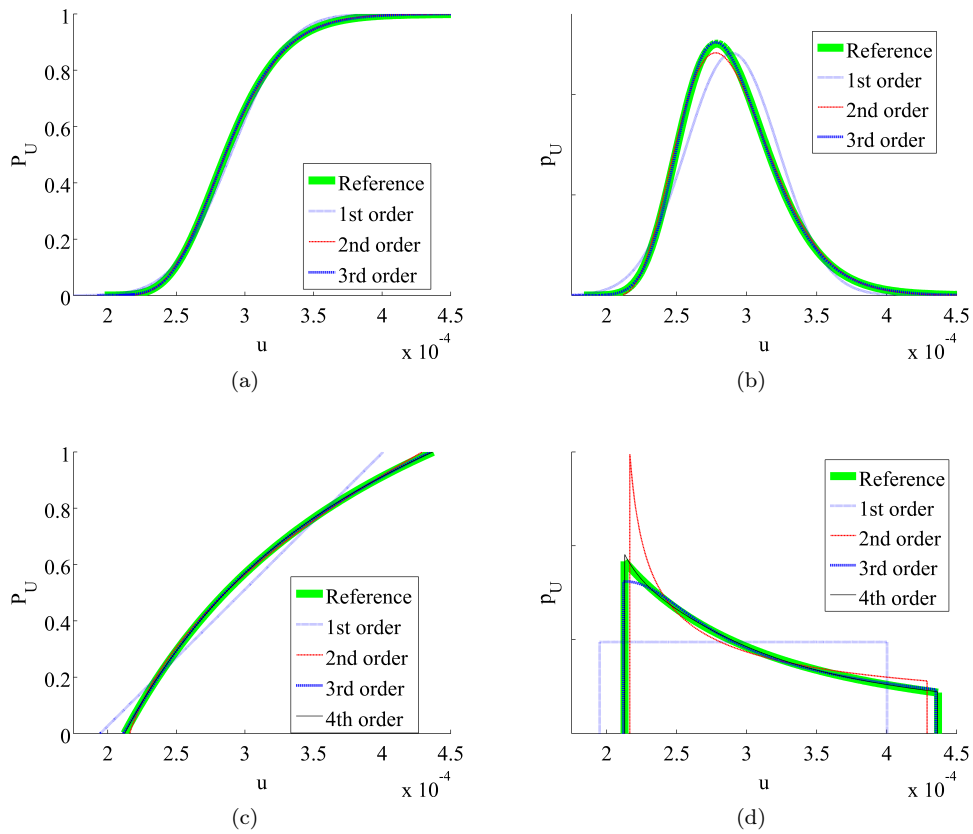

Figure 6: Displacement results obtained at null frequency (*i.e.* the static case) for different representation orders; empirical CDF (a) and PDF (b) for Hermite-Chaos for the Gaussian stiffness case; empiricals CDF (c) and PDF (d) for Legendre-Chaos for the uniform stiffness case.

The first numerical investigation with PC representation concerns the static case. This situation is the most common in the literature. Not surprisingly, Figure 6 shows that satisfactory results can be achieved at the 3-*rd* or the 4-*th* order. Moreover, regarding the convergence of the series, it is observed that the CDFs and PDFs approach better and better the reference curve from an order of expansion to the next one. This behavior for the CDF approximation is in accordance with theoretical results of PC representation. Moreover, from this figure, one can suppose that acceptable shapes for the PDF are obtained even when the convergence is not fully achieved. However, from the results reported in the following of this study, we can state that this behavior is only a consequence of the low order n_{U} required to get an accurate result.

Next, numerical investigations with PC representation concern the dynamic case. Then, the error ϵ defined in Eq. (31) helps to quantify the representation quality for each frequency of the range of interest and the three considered normalized coefficients of variation. Empirical inverse CDFs of the distributions obtained from the PC expansion are compared to the empirical inverse CDFs and the empirical variances of the reference produced by Monte Carlo simulations with 10^6 sample size. It is stated that a satisfactory representation is achieved when ϵ is less than or equal to $5 \cdot 10^{-4}$, meaning that the reference PDFs of the response U_ω agree well with the ones given by a PC representation. For this test, we limit arbitrarily the order of the expansion to the 70-*th* order. Considering the PC representation for the Legendre-uniform stiffness case, Figure 7 shows the empirical PDFs of real and imaginary parts of U_ω at the 65-*th* and 70-*th* orders for the natural frequency. Discrepancies are more visible for the real part: small fluctuations around reference PDF observed at the 65-*th* order disappear at the 70-*th* order. Errors are $\epsilon \simeq 1 \cdot 10^{-3}$ for the 65-*th* order and $\epsilon = 5 \cdot 10^{-4}$ for the 70-*th* order. So, the chosen ϵ criterion limit implies accurate results for the PDFs.

Figure 8 shows the order of truncation required to achieve a satisfactory representation of the PDFs using the above criterion for the two considered distributions for K. Results for the three cases of SDOFs systems studied are represented over the normalized frequencies. Normalized frequency is defined by the ratio between the true frequency f and the eigenfrequency f_0 of the nominal SDOF system. First, we can note that the PC representation performs globally better for the uniform stiffness case than the one for the Gaussian stiffness case. As it is expected, very satisfactory results are obtained at high frequency (saying the normalized frequency equals two in the current example) with an expansion truncated at the 4-*th* order, whatever the chosen damping level is. For the Gaussian stiffness case, looking at the PDFs of the real and the imaginary parts of U_ω on logarithmic scale shows that the last two coefficients of the Hermite representation help only to well adjust the tails of the distributions. For the high damping case η_1, it is found that an order expansion less than ten suffices for a good representation over the complete frequency range and especially around the resonant frequency of the nominal system in both stiffness distributions cases. For the medium damping case η_2 and around the resonant frequency of the nominal system, the PC representation:

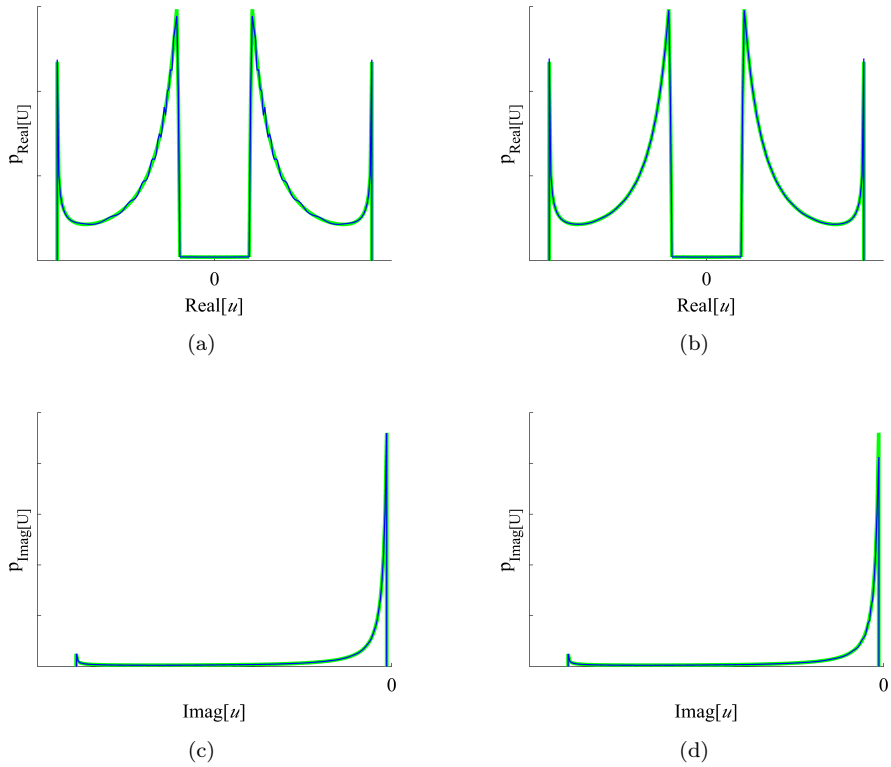

Figure 7: Comparison of empirical PDFs obtained for U_ω using a Legendre basis representation at the natural frequency of the nominal system for η_3 in the uniform stiffness case; thick green curves are for the reference, light black curves are for the PC representation; (a) real part at 65-*th* order; (b) real part at 70-*th* order; (c) imaginary part at 65-*th* order; and (d) imaginary part at 70-*th* order.

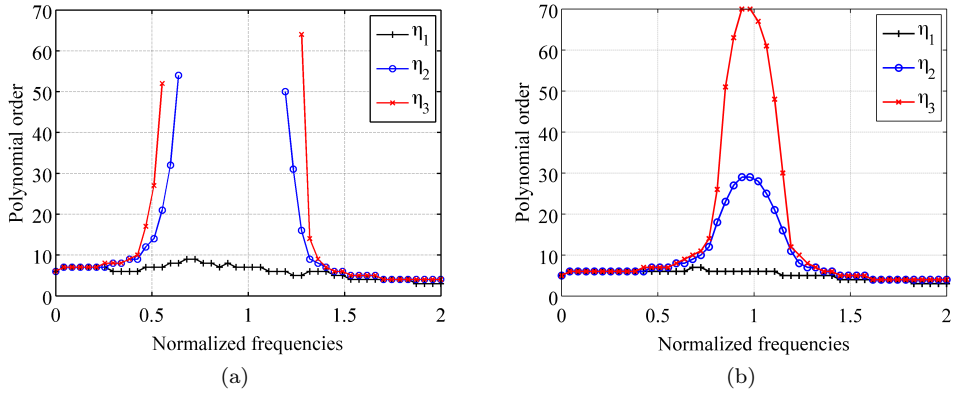

Figure 8: Order of polynomial required versus normalized frequencies to satisfy $\epsilon \leq 5 \cdot 10^{-4}$ for the representation of the SDOF response when considering the three damping ratios η_m, $m \in \{1, 2, 3\}$; Subfigure (a) concerns the Hermite-Chaos for the Gaussian stiffness case while subfigure (b) concerns the Legendre-Chaos for the uniform stiffness case.

- does not lead to convergence for the Gaussian stiffness case when the polynomial order is limited to the 70-*th* order,
- requires a 29-*th* order for the uniform stiffness case.

For the low damping η_3, results are worse in both cases, the uniform stiffness case requires up to a 70-*th* order to get accurate results in a region around the resonant frequency on the graph. This can be explained by a very poor convergence of the expansion for the SDOF response at these frequencies for such a normalized coefficient of variation. This phenomenon has also been observed and analyzed in [30]; the same authors later proposed a scheme to accelerate the convergence of the first two moments in [31]; however, in these works, no attention is paid to the PDFs.

To gain insight into such a failure of the PC representation for the Hermite-Gaussian stiffness case, Figure 9 shows the empirical CDFs and PDFs of real and imaginary parts obtained for U_ω at the 70-*th* order, considering the unitary normalized frequency. In this situation, $\epsilon \simeq 0.1$. It is observed that both obtained CDFs fluctuate around references CDFs, with many oscillations and inflections points. They are easily revealed by the observation of both PDFs. This observation differs from the one made for the static case where it has been observed that the PDFs of a non converged expansion is anyhow closed to the reference curve. This is a consequence of using very high orders: There are many spurious peaks, and they do not reflect the real ones, since they do not occur systematically at the correct location. Another comment concerns boundaries of these functions. Discrepancies occur if we look at their extrema. This is even a major problem for the distribution of the imaginary part since it has a tail fragment into the positive values region of the displacements.

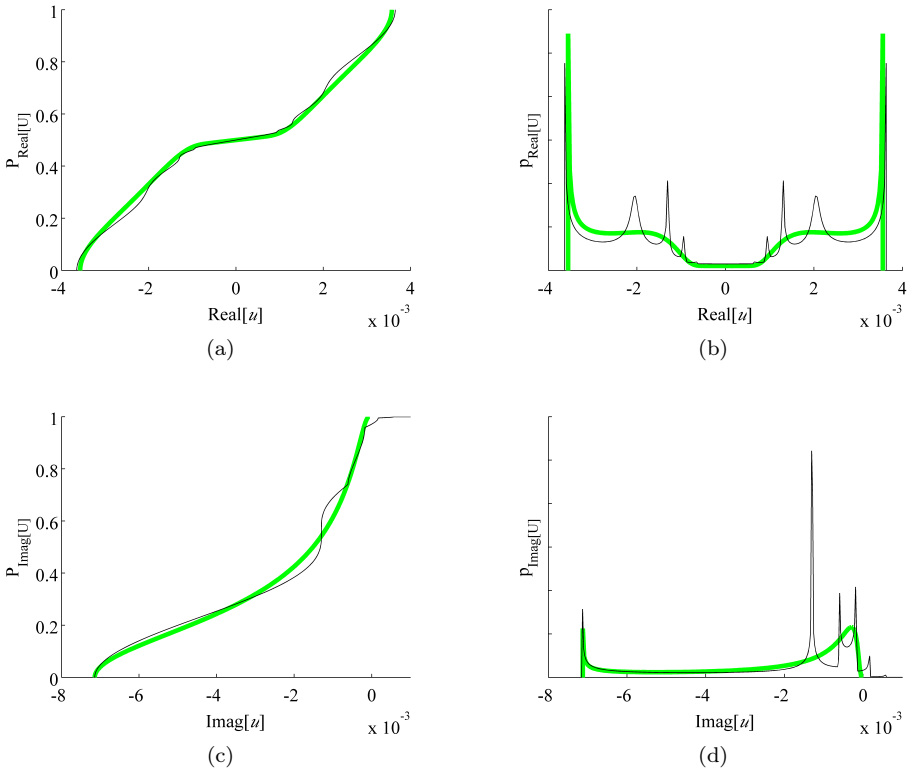

Figure 9: Comparison of empirical CDFs of (a) real and (c) imaginary parts and PDFs of (b) real and (d) imaginary parts obtained for U_ω with a 70-th order representation using an Hermite basis at the natural frequency of the nominal system for η_3 in the Gaussian stiffness case; thick green curves are for the reference, light black curves are for the PC representation.

3.2. PC representations onto other bases

3.2.1. Using standard PC bases representation

To cope with a satisfactory representation of the response when a high normalized coefficient of variation characterizes the system of interest, the simplest idea is to try other polynomial bases. Since it is a continuous distribution, Legendre, Laguerre and Chebyshev polynomials are first candidates. Thus, focusing on results when considering η_3 at the unitary reduced frequency, we can find some situations where other polynomial bases lead to better results.

For instance, when considering η_3 and the unitary reduced frequency, better results are obtained by a non intrusive approach (Eq. (13) for $Z = U_\omega$ and $z_r = u_r$) using:

- the Legendre basis truncated at the n_{U} =31-*st* order for the Gaussian stiffness case, and
- the Chebyshev of 1-*st* kind basis truncated at the n_{U} =47-*th* order for the uniform stiffness case.

To be complete, isoprobabilistic transformations $\mathcal{T}_{\mathrm{K}}(x) = P_{\mathrm{K}}^{-1}\left(P_{\mathrm{X}}(x)\right)$ are used in both these situations. According to Table 2, the input variable X is chosen uniform when using the orthonormal Legendre basis. In such a situation, the Gaussian stiffness is given by:

$$K = \mu_{\mathrm{K}} + \sigma_{\mathrm{K}}\sqrt{2}\mathrm{erf}^{-1}\left(X\right). \tag{32}$$

But when using the orthonormal Chebyshev of 1-*st* kind basis, $p_X = \frac{1}{\pi\sqrt{1-x^2}}$ (see Table 2). In this situation, the Gaussian stiffness is expressed by:

$$K = \mu_{\mathrm{K}} + \sigma_{\mathrm{K}}\frac{2\sqrt{3}}{\pi}\arcsin\left(X\right). \tag{33}$$

That said, an intrusive approach is desirable since our mechanical problem is linear. First attempts consist in using the standard intrusive method introduced above, Eq. (28), in conjunction with a Legendre polynomial basis for the Gaussian stiffness case and in conjunction with a Chebyshev of 1-*st* kind basis for the uniform stiffness case. Unfortunately, this does not lead to any good results if we keep the order n_{K} lower or equal to n_{U}. Explanation comes from the fact that choosing the same polynomial basis for the representation of K and for the representation of U_ω is not an adequate choice. Indeed, the random variable K is not efficiently represented in both the above considered cases, as it is shown in Figure 10 where the PC representation of K is plotted for the order $n_{\mathrm{K}} = n_{\mathrm{U}}$. In both cases, even if the CDFs of K seem good enough at the order chosen, one can see that the PDFs exhibit a ripple phenomena, indicating that convergence is not truly achieved. Then, a simple remedy would be to increase the number of terms for the representation of K in this situation. For instance, when considering the Gaussian stiffness case, numerical experiences suggest to select $n_{\mathrm{K}} = 43$ and $n_{\mathrm{U}} = 37$ when using the Legendre basis, according to the ϵ criterion.

For an intrusive approach, it is clear that the two bases intrusive method proposed above, Eq. (27), performs better than the standard intrusive method for the considered situations. Hence, by using:

- the Legendre basis truncated at the n_{U} =31-*st* order for ψ_q, and the Hermite basis truncated at the $n_{\mathrm{K}} = 1$-*st* order for ϕ_r in the Gaussian stiffness case[2];
- the Chebyshev of 1-*st* kind basis truncated at the n_{U} =47-*th* order for ψ_q, and the Legendre basis truncated at the $n_{\mathrm{K}} = 1$-*st* order for ϕ_r in the uniform stiffness case[3];

results of the intrusive method are recovered for the situations investigated. By using two different bases in the same appropriate formulation, one to represent the random variable K and another one to represent the output variable U_ω, it becomes possible to keep the two truncature orders as low as possible. Notice however that such a way leads to a higher numerical cost than the classical – one single basis – non-intrusive approach since the quadrature formula necessitates more integration points while more non-zeros terms stay within matrices. But, in this way, results of the non intrusive approach are recovered with the intrusive one. Same results are also obtained with Eq. (23).

However, for the current problem, although this two bases approach leads now to a satisfactory result, in contrast to the classical one with the standard bases, requiring such a high order is not a very efficient PC representation. More problematic is the fact that the alternate bases are found to be even less effective for expanding U_ω for low or high frequencies or for a lower normalized coefficient of variation, requiring truncature orders greater than 70th. In practice, it would not be desirable to change the representation basis to cover all the frequency range of interest, since it becomes very difficult to manage it when a multi degrees of freedom system will be concerned. Hence, a compound basis would be a preferable solution, at the expense of an increase of the number of terms in the representation chosen, since it is more important to cover all the range of frequencies. It is the subject of the next subsection.

[2]To be more precise for this situation, orthonormal Legendre polynomials are chosen for the basis $\mathbf{\Psi}(X)$, so the input variable X is chosen uniform, and an isoprobabilistic transformation $\mathcal{T}_{\mathrm{Y}}(x) = P_{\mathrm{Y}}^{-1}(P_{\mathrm{X}}(x))$ is introduced to evaluate the Hermite polynomial basis $\mathbf{\Phi}(\mathcal{T}_{\mathrm{Y}}(X))$, such that:

$$\mathcal{T}_{\mathrm{Y}}(x) = \sqrt{2}\mathrm{erf}^{-1}(x)$$

[3]To be more precise for this situation, Chebyshev of 1-*st* kind polynomials are chosen for the basis $\mathbf{\Psi}(X)$, so $p_X = \frac{1}{\pi\sqrt{1-x^2}}$, and an isoprobabilistic transformation $\mathcal{T}_{\mathrm{Y}}(x) = P_{\mathrm{Y}}^{-1}(P_{\mathrm{X}}(x))$ is introduced to evaluate the Legendre polynomial basis $\mathbf{\Phi}(\mathcal{T}_{\mathrm{Y}}(X))$, such that:

$$\mathcal{T}_{\mathrm{Y}}(x) = \frac{2\sqrt{3}}{\pi}\arcsin(x)$$

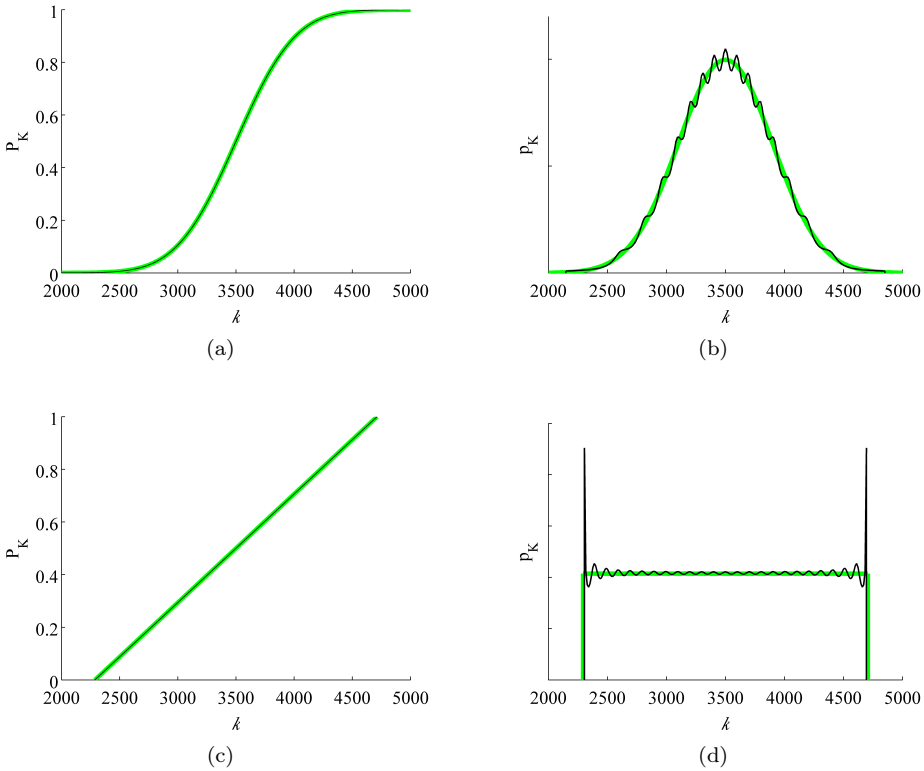

Figure 10: Comparison of empirical (a) CDF and (b) PDF obtained for Gaussian stiffness K with a 31-*st* order representation using a Legendre basis; (c) CDF and (d) PDF obtained for uniform stiffness K with a 47-*th* order representation using a Chebyshev of 1-st kind basis; thick green curves are for the reference, thin black curves are for the PC representation.

3.2.2. Using a mixed PC basis representation

From the previous results, it is desirable to find a way for enhancing the polynomial basis chosen for the representation of the random response. Enrichment basis strategy of reference [14] seems an attractive way, since it is complementary to the current formulation. Unfortunately, when using the same enrichment than that are proposed in reference [14] for our SDOF application, slightly improved results can be found but they are not tremendous: the orders required to satisfy the criterion are lower than, at most, four.

From the results of the previous subsection, our proposal is to have a compound representation basis made from the mix of two bases that has been found to be effective in all the range of frequencies for the random variable. Hybrid formulation is not new since it is found in literature for SRBM based on stochastic Krylov subspace (see reference [16]). But the strict application of SRBM does not help for the application concerning a SDOF system. Indeed, the complete basis of Krylov subspace has a fixed dimension given by the number m of degrees of freedom of the mechanical system. It is $m = 1$ in our SDOF system. Without conditioning, the first vector of the Krylov subspace is made from the force vector which is $q = 1$ here. Thus, for the SDOF application, our proposal is rather to use a compound basis, made from the two bases which have been found effective previously. Since two bases are involved to represent a single random variable in this strategy, we call it a mixed PC basis representation. This is different from the two bases strategy of the previous subsection, since only one basis is used for both random variables.

From a mathematical point of view, it is obvious that compounding two bases forms a spanning set. In practice, it can be made by forming the product of all polynomials pertaining to both bases. With such a strategy, a curse of dimensionality arises rapidly, which forces us to have very low truncation orders for the underlying bases. Our numerical experience shows that this does not lead to satisfying results for the SDOF response problem. Concatenating simply the two initial bases is another possibility of interest. This leads to represent U_ω as usually in PC methods with $U_\omega = \mathbf{\Psi u}$ but for:

$$\mathbf{\Psi} = \left\{1,\, \Psi_1^{(\mathcal{A})},\, \cdots,\, \Psi_{n_A}^{(\mathcal{A})},\, \Psi_1^{(\mathcal{B})},\, \cdots,\, \Psi_{n_B}^{(\mathcal{B})}\right\}. \tag{34}$$

if we denote now $\Psi_i^{(\mathcal{A})}$ and $\Psi_j^{(\mathcal{B})}$ the polynomials of two bases $(\mathcal{A})$ and $(\mathcal{B})$, such as Hermite and Legendre polynomials, or Legendre and Chebyshev of 1-*st* kind polynomials, for example. Orders of truncature are n_A and n_B for the bases $(\mathcal{A})$ and $(\mathcal{B})$, respectively. This corresponds to a drastic selection of the terms which are produced in the previous strategy, but it enables to keep higher orders terms of both bases for numerical investigations. A consequence of such a simple strategy is the non uniqueness of the basis coefficients for one given representation. Moreover, the sparsity of the matrix $\mathcal{K}$ involved in Eq. (25) is deteriorated. Both of these consequences are due to an uninvolved orthogonality strategy for the spanning set construction. This can increase the necessary amount of memory and this can induce a difficulty if we want to have an

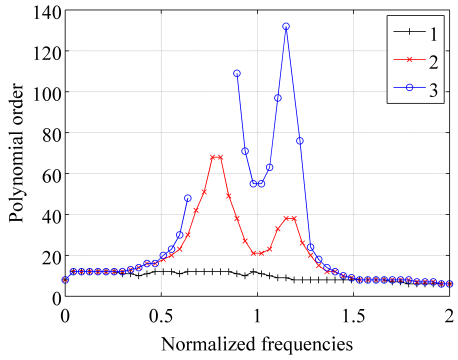

Figure 11: Polynomial order (index in the set defined in Eq. (35)) versus normalized frequencies for the representation onto a mixed, Hermite-Legendre polynomial basis of the SDOF response when considering the three damping ratios η_m, $m \in \{1, 2, 3\}$.

optimized, reduced set, with a minimal truncature order in the end. But our objective is mainly to test if a successful PC representation of U_ω can be achieved through this strategy.

For numerical investigations we focus on the Gaussian stiffness case since it is the more critical case. From the observations of the previous subsection, the mixed basis is chosen to be composed of Hermite and Legendre polynomials. When considering the η_2 damping ratio, satisfying results are achieved by choosing either $n_A = 50$ and $n_B = 20$ or $n_A = 35$ and $n_B = 35$, illustrating the non uniqueness of PC representations for U_ω by this strategy. To assess the global efficiency of this strategy over all the range of frequencies for the three damping ratios, we have set $n_A = 70$ and $n_B = 70$ and reordered the polynomial set terms such that:

$$\mathbf{\Psi} = \left\{1,\, \Psi_1^{(\mathcal{A})},\, \Psi_1^{(\mathcal{B})},\, \cdots,\, \Psi_{70}^{(\mathcal{A})},\, \Psi_{70}^{(\mathcal{B})}\right\}. \tag{35}$$

This enables us to report the order of truncation necessary to respect the defined criterion; the "order" here denotes the index in the set. This is given in Figure 11. By comparing this figure with Figure 8(a), one can see that an improvement is achieved around the resonant frequency for the medium and the high damping situations. But it is also found that this strategy is not completely satisfying since it again exists a range of frequencies for which no satisfying results are obtained for the high damping situation -corresponding to the blue curve for both of these figures- between the low frequencies and the resonant frequency. Difficulties persist to represent the imaginary part of the response in this frequencies range where a very narrow spread of the PDF with very small values is exhibited.

3.2.3. Using an output variable based basis

From the previous experiments and analytical results given in [18, 19, 21], we can assume that the set of orthogonal polynomials would be different along frequencies. But for the SDOF system, we have found that standard polynomial bases are adequate for the

null frequency response. Then, when progressing in a frequency sweep and approaching resonant frequencies, these polynomials appear less and less adequate, and one can think that they should be replaced by new, more adequate bases. Thus, in a frequency sweep, as the PC representation for the response at previous frequencies has been obtained, this known response can be an optimal candidate for a judicious random variable in PC. For instance, when the output variable U_{ω_k} becomes of interest while the representation of the output variable $U_{\omega_{k-1}}$ is already determined, one can generate a new polynomial basis from the zero-mean random variable $X = U_{\omega_{k-1}} - \mathrm{E}\left[U_{\omega_{k-1}}\right]$. In this work, the proper basis is constructed numerically by using a Gram-Schmidt orthogonalization procedure, followed by a normalization step as described in Algorithm 1 (see also appendix A of reference [3] dedicated to orthogonal expansions for random process). This leads to satisfy $\psi_0(x) = 1$ and:

$$\int_{x\in\mathcal{D}} \psi_r^*(x)\,\psi_q(x)\,p_{\mathrm{X}}(x)\,\mathrm{d}x = \begin{cases} 0 & \text{if} \quad r \neq q \\ 1 & \text{if} \quad r = q \end{cases} \tag{36}$$

where $\bullet^*$ stands for complex conjugate and where MCS is involved to evaluate these integrals. Hence, updating the polynomial basis along the frequency sweep enables to reduce the non-linearity degree of the representation problem at the investigated frequency by transforming it to a new random variable given at the previous frequency.

Data: $U_{\omega_{k-1}}$, output variable for ω_{k-1} circular frequency;
$\psi_0 \leftarrow 1$;
$X \leftarrow U_{\omega_{k-1}} - \mathrm{E}[U_{\omega_{k-1}}]$;
for $r \leftarrow 1$ **to** n_U **do**
  $\psi_r \leftarrow X^r - < \psi_{r-1}, X^r > \psi_{r-1}$;
  $\psi_r \leftarrow \frac{1}{\sqrt{<\psi_r^\star, \psi_r>}}\psi_r$;
end

Algorithm 1: Procedure for building the output variable based basis $\mathbf{\Psi}$ when an output variable $U_{\omega_{k-1}}$ is known.

Several strategies can be thought to decide when it becomes necessary to update the polynomial basis. For extremely simple problems, one of them can be given by the condition:

$$\max_{q>1}\left(|u_q|\right) \geq \alpha\,|u_1| \tag{37}$$

where values given to q are linked to a chosen maximum polynomial order for the representation and where α is a predefined threshold value (typically 10^{-5}). For example, if a third order truncation is desired, we have to update the polynomial basis if $\max\left(|u_q|\right) \geq \alpha\,|u_1|$ for $q > 3$. For more complex problems, a more robust strategy to update the polynomial basis may be needed if the necessary order exceeds the predefined order, when ensuring convergence of the PC representation through the use of the error indicator proposed in subsection 2.2.

In order to made comparable all results of this work, we chose here another strategy to update the polynomial basis. It consists in updating the polynomial basis at each

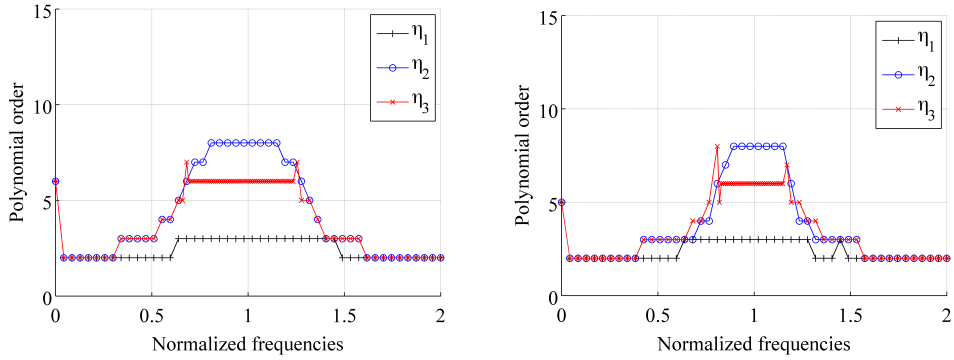

Figure 12: Order of "output variable based" polynomial required versus normalized frequencies to satisfy $\epsilon \leq 5 \cdot 10^{-4}$ for the representation of the SDOF response when considering the three damping ratios η_m, $m \in \{1, 2, 3\}$; Subfigure (a) concerns the Gaussian stiffness case while subfigure (b) concerns the uniform stiffness case.

new frequency ω_{k+1} based on the response at the previous frequency ω_k. However, if a representation order greater to 8 appears to be necessary, the frequency increment is reduced, dividing it by a factor 2. Results are shown in figure 12 where the initial basis at null frequency is constituted by Hermite polynomials for the Gaussian stiffness distribution, while Legendre polynomials are chosen for the uniform distribution. It can be observed that order 8 becomes now sufficient for η_1 and η_2 by using such "output variable based" bases. However, for η_3, it is necessary to reduce the frequency increment near the resonant frequency in order to not exceed the 8-*th* order for the truncation of the bases. As a consequence, for this damping, the number of studied frequencies increases by 85% for the Gaussian stiffness case while it is 40% for the uniform stiffness case.

One can conclude here that the output variable based polynomial representation can be a practical solution to address pitfalls in the polynomial chaos representation of frequency response of random SDOF mechanical systems, by updating the PC basis through frequencies, when an adequate basis can be found to start the frequency sweep. Although this strategy is inspired from the reference [3], it can also be seen as the frequency counterpart of the strategy involved for temporal problems addressed in reference [11].

3.2.4. Using a multi-element basis

A last test is performed which uses a piecewise expansion with low degree rather than a "one piece" expansion with high polynomial degree. As mentioned in the introduction, the idea was introduced a few years ago by [12, 13] and successfully applied to several mechanical problems [32, 33]. We will later denote this method by MEgPC for Multi-Element generalized Polynomial Chaos.

When considering a normal random variable to describe the random input K, an iso-probabilistic transformation is used to work with a uniform random variable ζ which

has a bounded range of values $\mathcal{I} = [-1, 1]$:

$$K = \mu_{\mathrm{K}} + \sigma_{\mathrm{K}} \mathcal{T}(\zeta), \quad \mathcal{T}(\zeta) := \sqrt{2}\mathrm{erf}^{-1}(\zeta) \tag{38}$$

When a uniform distribution is considered for K, this step is not necessary as it can be directly expressed using ζ:

$$K = \mu_{\mathrm{K}} + \sigma_{\mathrm{K}} \sqrt{3}\zeta \tag{39}$$

The range $\mathcal{I}$ is easy to cut into pieces, that is to be partitioned into n_e non-overlapping elements denoted $\mathcal{I}_n = (\zeta_b^{(n-1)}, \zeta_b^{(n)})$. Over each element, a polynomial expansion in a local ζ_n random variable is performed using a low degree – either in an intrusive or a non intrusive way. Local variables ζ_n follow a uniform law over $[-1, 1]$ and are linked to ζ via affine transformations $\zeta_n = \mathcal{T}_n(\zeta)$ with:

$$\mathcal{T}_n(\zeta) = \frac{2}{\zeta_b^{(n)} - \zeta_b^{(n-1)}} \left(\zeta - \frac{\zeta_b^{(n-1)} + \zeta_b^{(n)}}{2} \right), \ \zeta \in \mathcal{I}_n \tag{40}$$

Legendre polynomials in ζ_n are used to perform the expansion of U_ω over each $\mathcal{I}_n$ element; this local expansion is denoted $U_{\omega,n}(\zeta_n)$ and is such that:

$$\mathrm{Prob}[U_{\omega,n} \leq x] = \mathrm{Prob}[U_\omega \leq x \,|\, \zeta \in \mathcal{I}_n] \tag{41}$$

Expansion coefficients are denoted $u_{q,n}$ where q refers to the polynomial degree and n to the element index:

$$U_{\omega,n}(\zeta_n) = \sum_{q=0}^{n_{\mathrm{U}}-1} u_{q,n} \psi_q(\zeta_n) \tag{42}$$

U_ω probability can finally be evaluated as follows:

$$\begin{aligned} \mathrm{Prob}[U_\omega \leq x] &= \sum_{n=1}^{n_e} \mathrm{Prob}[U_\omega \leq x \cap \zeta \in \mathcal{I}_n] \\ &= \sum_{n=1}^{n_e} \mathrm{Prob}[U_\omega \leq x | \zeta \in \mathcal{I}_n] \ \mathrm{Prob}[\zeta \in \mathcal{I}_n] \\ &= \sum_{n=1}^{n_e} \mathrm{Prob}[U_{\omega,n} \leq x] \frac{\zeta_b^{(n)} - \zeta_b^{(n-1)}}{2} \end{aligned} \tag{43}$$

An important question is the choice of $\mathcal{I}_n$ elements. Adaptive strategies can be implemented to recursively refine the partition based on a given criterion [12, 34, 35]. Here, the partition will be set *a priori* and the quality of the global expansion will be measured by ϵ. The obvious partition consists in n_e elements with same size $2/n_e$. This type of partition is used in the uniform stiffness case. However, this gives no good result in the Gaussian stiffness case: due to the isoprobabilistic transformation, side elements $[-1, -1+2/n_e]$ and $[1-2/n_e, 1]$ account for "large" – indeed infinite – elements in the image space $\mathcal{T}(\zeta)$. Hence, the Gaussian tails are poorly represented. The chosen partitions are then built arbitrarily as follows:

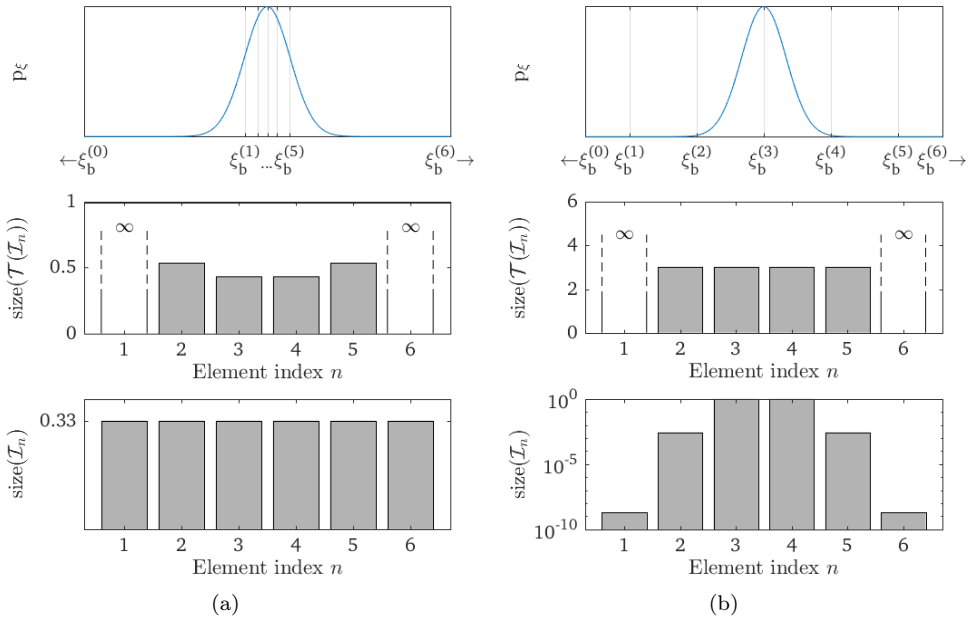

Figure 13: Illustration of the partitions obtained when using $n_e = 6$ elements $\mathcal{I}_n$ with a constant size (a) or with boundaries defined by Eq. (44) (b). $\xi_b^{(n)} = \mathcal{T}(\zeta_b^{(n)})$ denote elements boundaries in the Gaussian variable space.

$$\mathcal{I}_n = [\zeta_b^{(n-1)}; \zeta_b^{(n)}],\ 1 \leq n \leq n_e \qquad (44)$$
$$\text{with} \begin{cases} \zeta_b^{(0)} = -1,\ \zeta_b^{(n_e)} = +1 \\ \zeta_b^{(n)} = \mathcal{T}^{-1}(-6 + (n-1)\frac{12}{n_e - 2}),\ 1 \leq n \leq n_e - 1 \end{cases}$$

An illustration of such a partition compared to a constant size elements partition is displayed in Figure 13. When using elements with equal size in ζ, most of them account for central values for ξ (close to the mean). Using a partition defined by Eq. (44), the size of elements in ξ (that is size($\mathcal{T}(\mathcal{I}_n)$)) is constant except for the first and last elements which are of infinite size.

The global procedure used to compute the multi-element expansion of U_ω in the case of a Gaussian random input is provided in Algorithm 2. The procedure to compute the realization value u_ω for a given realization k of K is described in Algorithm 3.

Figure 14 shows the minimal number of elements required to satisfy the criterion using a degree 5 expansion over each element; a non intrusive evaluation of the coefficients is used. As can be seen, the MEgPC method provides a mean to get an accurate representation for all three values of η and all over the frequency range. As expected, the Gaussian stiffness case requires generally more elements to satisfy the accuracy criterion as the relationship between a Gaussian and a uniform distribution is very non linear. The computational effort here is proportional to the number of elements: $n_e \times 6$ coefficients have to be evaluated (using a 5-th order expansion). Compared to a classical

Data:
n_e, number of elements;
$(\psi_i)_{0\leq i\leq n_{\mathrm{U}}-1}$, family of n_{U} orthogonal Legendre polynomials;
$(x_i)_{1\leq i\leq n_{\mathrm{G}}}$ and $(w_i)_{1\leq i\leq n_{\mathrm{G}}}$, nodes and weights of the quadrature rule used for the Legendre polynomials and its associated inner product.

for $n \leftarrow 0$ **to** n_e **do** `// Partition definition`
  Compute $\zeta_b^{(n)}$ according to Eq. (44);
end
for $n \leftarrow 1$ **to** n_e **do** `// Local expansion over each element`
  for $i \leftarrow 1$ **to** n_{G} **do** `// Values at nodes`
    $g_i \leftarrow g(\mu_K + \sigma_K \mathcal{T}(\mathcal{T}_n^{-1}(x_i)); \omega)$;
  end
  for $q \leftarrow 0$ **to** $n_{\mathrm{U}} - 1$ **do** `//` $U_{\omega,n}(\zeta_n)$ `expansion coefficients`
    $u_{q,n} \leftarrow \sum_{i=1}^{n_{\mathrm{G}}} w_i \psi_q(x_i) g_i$;
  end
end

Algorithm 2: Algorithm to compute MEgPC exapnsion in the case of a Gaussian random input

Data:
k, value of K realization;
$(\zeta_b^{(n)})_{0\leq n\leq n_e}$, elements boundaries;
$(\psi_i)_{0\leq i\leq n_{\mathrm{U}}-1}$, family of n_{U} orthogonal Legendre polynomials;
$(u_{q,n})_{0\leq q\leq n_{\mathrm{U}}, 1\leq n\leq n_e}$, local expansions coefficients for U_ω.

$\xi \leftarrow (k - \mu_{\mathrm{K}})/\sigma_{\mathrm{K}}$;
$\zeta \leftarrow \mathcal{T}^{-1}(\xi)$;
Find n such that $\zeta \in \mathcal{I}_n$;
$\zeta_n \leftarrow \mathcal{T}_n(\zeta)$;
$u_\omega \leftarrow \sum_{q=0}^{n_{\mathrm{U}}-1} u_{q,n} \psi_q(\zeta_n)$;

Algorithm 3: Algorithm to evaluate u_ω realization given k value and U_ω MEgPC expansion

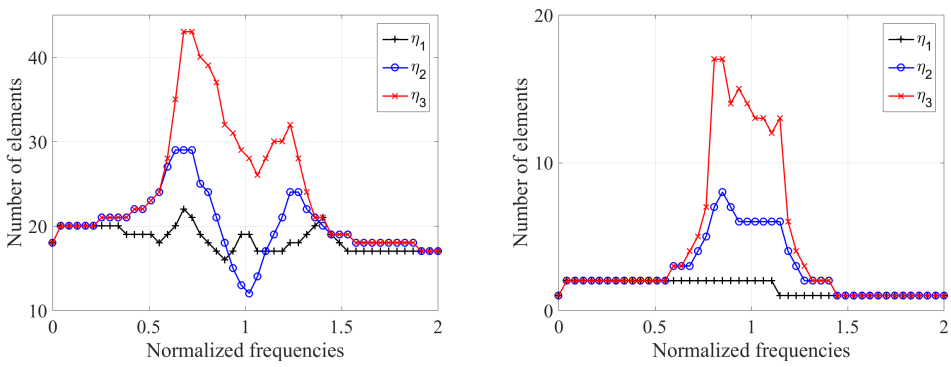

Figure 14: Number of elements required versus normalized frequencies to satisfy to satisfy $\epsilon \leq 5 \cdot 10^{-4}$ for the MEgPC representation of the SDOF response when considering the three damping ratios η_m, $m \in \{1, 2, 3\}$; Subfigure (a) concerns the Gaussian stiffness case while subfigure (b) concerns the uniform stiffness case.

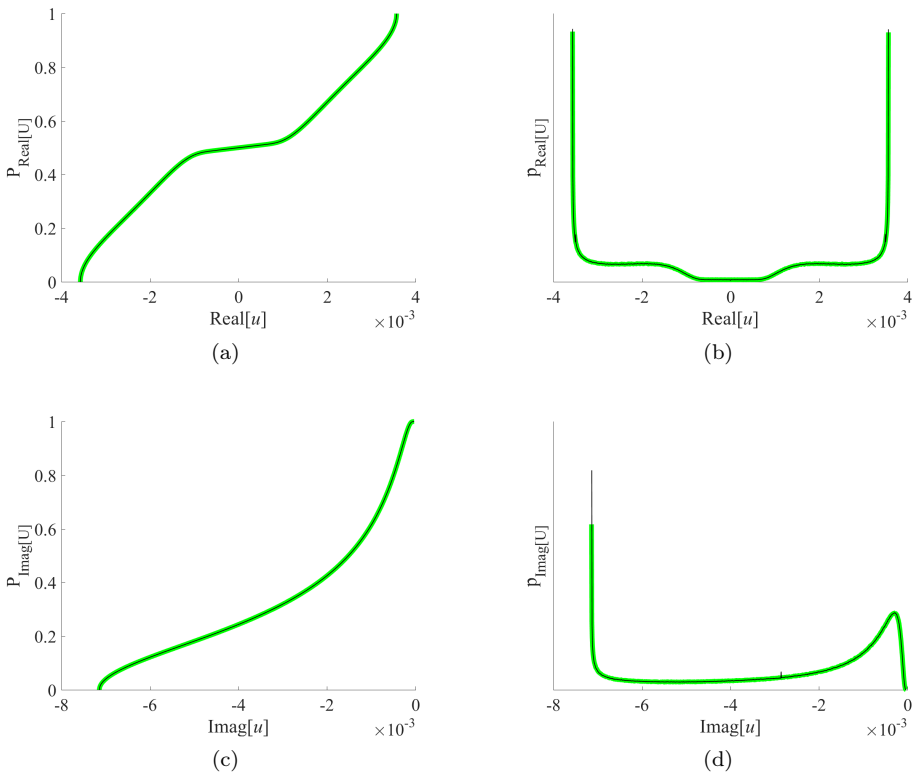

Figure 15: Comparison of empirical CDFs of (a) real and (c) imaginary parts and PDFs of (b) real and (d) imaginary parts obtained for U_ω with a 5-th order MEgPC representation using 30 elements at the natural frequency of the nominal system for η_3 in the Gaussian stiffness case; thick green curves are for the reference, light black curves are for the PC representation.

"one-piece" PC representation, it means that a collection of n_e small systems have to be solved in this case instead of a large system. In the case of a non intrusive evaluation of the coefficients, having low degrees over each element means that fewer points are required for the quadrature, but these values at quadrature nodes have to be evaluated for each element. Most importantly, it preserves low degrees for the expansion and thus prevents from bad conditioning and Gibbs phenomenon.

Figure 15 describes the CDF and PDF of real and imaginary parts of U_ω at the natural frequency of the nominal system for η_3. 30 elements are required to satisfy the accuracy criterion. As showed by the figure, the CDF and the PDF returned by the expansion perfectly fit the reference curves.

Conclusion

While many studies focus on the handling of finite element models which have an increasing complexity as well as a large number of kinematic degrees of freedom and a large number of random variables, we focus here on the effectiveness of the stochastic representation for the most simple, linear, system having one single degree of freedom

with only one random variable. The stiffness is the input random variable, while the system response is the random output of the problem. The simplicity of the chosen situation enables the access with high fidelity to the expected results in order to gain insight to the PC representation process. For SDOF systems, the numerical cost involved by PC representation is not relevant since MCS is very efficient in this situation, so it is not discussed in this work. The purpose of the study is rather to investigate the effectiveness of the stochastic bases for the representation of the dynamic response, hoping results found here will be useful for more general situations, involving multiple-degrees-of-freedom stochastic dynamic systems.

First of all, it is shown that the frequency response distribution functions strongly depend on a normalized coefficient of variation, being defined as the coefficient of variation of the random stiffness variable divided by the modal damping ratio of the nominal mechanical system. Then, for the experimentation on dynamical systems, we have chosen to fix the stiffness coefficient of variation while damping is varied. It appears that stochastic responses become highly non-linear when reaching the resonant frequencies for a moderate to high normalized coefficient of variation.

To address these stochastic problems numerically from the PC representation, we have provided brief recalls over the PC methodology with its numerical implementation in order to discuss alternative strategies for this methodology. In addition, an error indicator based on the inverse CDF is defined. It is used in this work to assess for the quality of the representation of the random variable, but it is emphasized that this indicator also enables to assess convergence of the PC representation.

Experiments showed that standard polynomial bases fail to represent stochastic responses around the resonant frequencies, since unreasonable truncation order becomes necessary in practice. Hence, it appears that the optimal basis for the input variable can be far to be the optimal one for the output variable if a high degree of non linearity between both of them is encountered. In these conditions, the representation of the output random variable can be very difficult when using the basis chosen for the input variable.

Hence, a first proposed remedy to keep low the orders of expansion was the use of two bases, one for the input variable and another one for the output variable. This strategy is able to achieve accurate results but in an inefficient way. Hence, another strategy involving two bases was tested: the compound bases. It combines two standard polynomials bases to form a mixed basis. It seems to be particularly interesting since it would be adapted to the investigated situation as it uses the optimal basis for the input, known, random variable for the representation of the system output. From this strategy of compounding two bases, the representation appears to be more practical at only some frequencies ranges, namely the low, resonant and high frequencies but not around the resonant frequency in the addressed examples.

As a consequence, the next remedy tested was the continuous adaptation of the representation basis along the frequency sweep, when starting from standard bases. This

appears to be an efficient remedy for the situations tested. Finally, a multi-element PC representation was investigated. It is a robust approach in the sense that it can handle every situation without numerical difficulties since expansion order can be kept low by adding elements with smaller sizes. Both these last approaches are appealing to tackle dynamic responses of SDOF systems as they were shown to be effective, at least for the situations investigated in the current work. Advice which results from this study is then to use one of these last two methods when considering more general dynamical systems.

Funding

This research did not receive any specific grant from funding agencies in the public, commercial, or not-for-profit sectors.

References

[1] Norbert Wiener. The homogeneous chaos. *American Journal of Mathematics*, 60(4):897–936, 1938.

[2] P. B. Nair and A.J. Keane. Stochastic reduced basis methods. *AIAA Journal*, 40(8):1653–1664, 2002.

[3] S.R. Winterstein. Moment-based hermite models of random vibration. Technical Report 219, Dept. of Structural Engineering, Technical University of Denmark, Lyngby, Denmark, 1987.

[4] S.R. Winterstein. Nonlinear vibration models for extremes and fatigue. *Journal of Engineering Mechanics*, 114(10):1772–1790, October 1988.

[5] R.G. Ghanem and P.D. Spanos. *Stochastic Finite Elements A Spectral Approach*. Springer New York, 1991.

[6] D. Xiu and G.Em. Karniadakis. The Wiener-Askey polynomial chaos for stochastic differential equations. *SIAM J. Sci. Comput.*, 24(2):619–644, 2002.

[7] R. Askey and J. Wilson. *Some basic hypergeometric orthogonal polynomials that generalize Jacobi polynomials*, volume 54. American Mathematical Society, Memoirs of the American Mathematical Society edition, 1985.

[8] Oliver G. Ernst, Antje Mugler, HansJorg Starkloff, and Elisabeth Ullmann. On the convergence of generalized polynomial chaos expansions. *ESAIM Mathematical Modelling and Numerical Analysis*, 46:317–339, 3 2012.

[9] Dongbin Xiu, Didier Lucor, C.H. Su, and George Karniadakis. Performance evaluation of generalized polynomial chaos. In PeterM.A. Sloot, David Abramson, AlexanderV. Bogdanov, YuriyE. Gorbachev, JackJ. Dongarra, and AlbertY. Zomaya, editors, *Computational Science ICCS 2003*, volume 2660 of *Lecture Notes in Computer Science*, pages 346–354. Springer Berlin Heidelberg, 2003.

[10] D. Lucor, C.H. Su, and G. E. Karniadakis. Generalized polynomial chaos and random oscillators. *International Journal for Numerical Methods in Engineering*, 60(3):571–596, 2004.

[11] Marc Gerritsma, Jan-Bart van der Steen, Peter Vos, and George Karniadakis. Time-dependent generalized polynomial chaos. *Journal of Computational Physics*, 229(22):8333 – 8363, 2010.

[12] X. Wan and G.Em. Karniadakis. An adaptive multielement generalized polynomial chaos method for stochastic differential equations. *Journal of Computational Physics*, 209(2):617–642, 2005.

[13] X. Wan and G.Em. Karniadakis. Beyond Wiener-Askey expansions handling arbitrary PDFs. *Journal of Scientific Computing*, 27(13):455–464, 2006.

[14] Debraj Ghosh and Roger Ghanem. Stochastic convergence acceleration through basis enrichment of polynomial chaos expansions. *International Journal for Numerical Methods in Engineering*, 73(2):162–184, 2008.

[15] O.P. Le Maître and O.M. Knio. *Spectral Methods for Uncertainty Quantification*. Springer Netherlands, 2010.

[16] S.K. Sachdeva, P.B. Nair, and Keane A.J. Hybridization of stochastic reduced basis methods with polynomial chaos expansions. *Probabilistic Engineering Mechanics*, 21(2):182–192, 2006.

[17] P.S. Mohan, P.B. Nair, and A.J. Keane. Multi-element stochastic reduced basis methods. *Computer Methods in Applied Mechanics and Engineering*, 197(17–18):1495–1506, 2008.

[18] E. Pagnacco, R. Sampaio, and E. Souza de Cursi. Multimodality of the Frequency Response Functions of random linear mechanical systems. In *XXX CILAMCE Iberian Latin American Congress on Computational Methods in Engineering*, Rio de Janeiro, Brasil, November 08 to 11 2009.

[19] E. Pagnacco, R. Sampaio, and E. Souza de Cursi. Frequency response functions of random linear mechanical systems and propagation of uncertainties. *Mecanica Computacional*, XXX:3357–3380, 2011.

[20] E. Pagnacco, E. Sarrouy, R. Sampaio, and E. Souza de Cursi. Polynomial chaos for modeling multimodal dynamical systems - investigations on a single degree of freedom system. In Carlos G. Garcia Garino, Anibal E. Mirasso, Mario A. Storti, and Miguel E. Tornello, editors, *Mecanica Computacional XXXII:705-727*, 2013.

[21] Emmanuel Pagnacco, Rubens Sampaio, and Eduardo Souza de Cursi. Complexity of the response of linear systems with a random coefficient and propagation of uncertainties. *Journal of the Brazilian Society of Mechanical Sciences and Engineering*, 37(5):1591–1608, 2015.

[22] Eduardo Souza de Cursi and Rubens Sampaio. *Uncertainty Quantification and Stochastic Modeling with Matlab*. ISTE Press-Elsevier, 2015.

[23] E. Pagnacco, E. Souza de Cursi, and R. Sampaio. Subspace inverse power method and polynomial chaos representation for the modal frequency responses of random mechanical systems. *Computational Mechanics*, 58(1):129–149, 2016.

[24] V. Yaghoubi, S. Marelli, B. Sudret, and T. Abrahamsson. Sparse polynomial chaos expansions of frequency response functions using stochastic frequency transformation. *ArXiv e-prints*, June 2016.

[25] Y. K. Lin. *Probabilistic theory of structural dynamics*. McGrawHill, Inc., New York, 1967.

[26] F. E. Udwadia. Response of uncertain dynamic systems. i. *Applied Mathematics and Computation*, 22(23):115–150, May 1987.

[27] F. E. Udwadia. Response of uncertain dynamic systems. ii. *Applied Mathematics and Computation*, 22(23):151–187, May 1987.

[28] P. B. Nair and A.J. Keane. New developments in computational stochastic mechanics, part ii applications. In *41st AIAA/ASME/ASCE/AHS/ASC Structures, Structural Dynamics and Materials Conference*, Atlanta, GA, April 2000. AIAA. AIAA 2000-1441.

[29] H. Boistard. *Efficacité asymptotique de tests liés à la statistique de Wasserstein*. PhD thesis, University of Valladolid (Spain) and University of Toulouse 3 (France), 2007.

[30] E. Jacquelin, S. Adhikari, J-J. Sinou, and M. I. Friswell. Polynomial chaos expansion and steady-state response of a class of random dynamical systems. *Journal of Engineering Mechanics*, 141(4):04014145, 2015.

[31] E. Jacquelin, S. Adhikari, J-J. Sinou, and M. I. Friswell. Polynomial chaos expansion in structural dynamics: accelerating the convergence of the first two statistical moment sequences. *Journal of Sound and Vibration*, 356:144–154, 2015.

[32] Josselin Le Meitour, Didier Lucor, and Jean-Camille Chassaing. Prediction of stochastic limit cycle oscillations using an adaptive polynomial chaos method. *Journal of Aeroelasticity and Structural Dynamics, Vol 2, No 1 (2010)*, 2(1):3–22, 2010.

[33] E. Sarrouy, O. Dessombz, and J-J. Sinou. Stochastic study of a non-linear self-excited system with friction. *European Journal of Mechanics - A/Solids*, 40:1–10, 2013.

[34] E. Sarrouy, O. Dessombz, and J-J. Sinou. Piecewise polynomial chaos expansion with an application to brake squeal of a linear brake system. *Journal of Sound and Vibration*, 332:577–594, 2013.

[35] B. Chouvion and E. Sarrouy. Development of error criteria for adaptive multi-element polynomial chaos approaches. *Mechanical Systems and Signal Processing*, 66–67:201 – 222, 2016.